Molecular Therapy
Original Article

COVID-19-Induced ARDS Is Associated with Decreased Frequency of Activated Memory/Effector T Cells Expressing CD11a^{++}

Moritz Anft,[1,11] Krystallenia Paniskaki,[2,11] Arturo Blazquez-Navarro,[1,3,11] Adrian Doevelaar,[1] Felix S. Seibert,[1] Bodo Hölzer,[1] Sarah Skrzypczyk,[1] Eva Kohut,[1] Julia Kurek,[1] Jan Zapka,[1] Patrizia Wehler,[1,3] Sviatlana Kaliszczyk,[1] Sharon Bajda,[3] Constantin J. Thieme,[3] Toralf Roch,[1,3] Margarethe Justine Konik,[2] Marc Moritz Berger,[4] Thorsten Brenner,[4] Uwe Kölsch,[5] Toni L. Meister,[6] Stephanie Pfaender,[6] Eike Steinmann,[6] Clemens Tempfer,[7] Carsten Watzl,[8] Sebastian Dolff,[2] Ulf Dittmer,[9] Mohamed Abou-El-Enein,[3,10] Timm H. Westhoff,[1] Oliver Witzke,[2] Ulrik Stervbo,[1,11] and Nina Babel[1,3,11]

[1]Center for Translational Medicine and Immune Diagnostics Laboratory, Medical Department I, Marien Hospital Herne, University Hospital of the Ruhr University Bochum, Hölkeskampring 40, 44625 Herne, Germany; [2]Department of Infectious Diseases, West German Centre of Infectious Diseases, University Hospital Essen, University Duisburg-Essen, Hufelandstraße 55, 45147 Essen, Germany; [3]Berlin Institute of Health, Berlin-Brandenburg Center for Regenerative Therapies, and Institute of Medical Immunology, Charité-Universitätsmedizin Berlin, Corporate Member of Freie Universität Berlin, Humboldt-Universität zu Berlin, Augustenburger Platz 1, 13353 Berlin, Germany; [4]Department of Anesthesiology and Intensive Care Medicine, University Hospital Essen, University Duisburg-Essen, Hufelandstraße 55, 45147 Essen, Germany; [5]Department of Immunology, Labor Berlin GmbH, Sylter Straße 2, 13353 Berlin, Germany; [6]Department of Molecular and Medical Virology, Ruhr-University Bochum, Universitätsstrasse 150, 44801 Bochum, Germany; [7]Department of Gynecology and Obstetrics, Marien Hospital Herne, University Hospital of the Ruhr-University Bochum, Hölkeskampring 40, 44625 Herne, Germany; [8]Department of Immunology, Leibniz Research Centre for Working Environment and Human Factors at the Technical University Dortmund (IfADo), Ardeystrasse 67, 44139, Dortmund, Germany; [9]Institute for Virology, University Hospital Essen, University of Duisburg-Essen, Hufelandstraße 55, 45147 Essen, Germany; [10]Berlin Center for Advanced Therapies (BeCAT), Charité-Universitätsmedizin Berlin, Augustenburger Platz 1, 13353 Berlin, Germany

Preventing the progression to acute respiratory distress syndrome (ARDS) in COVID-19 is an unsolved challenge. The involvement of T cell immunity in this exacerbation remains unclear. To identify predictive markers of COVID-19 progress and outcome, we analyzed peripheral blood of 10 COVID-19-associated ARDS patients and 35 mild/moderate COVID-19 patients, not requiring intensive care. Using multi-parametric flow cytometry, we compared quantitative, phenotypic, and functional characteristics of circulating bulk immune cells, as well as SARS-CoV-2 S-protein-reactive T cells between the two groups. ARDS patients demonstrated significantly higher S-protein-reactive CD4$^+$ and CD8$^+$ T cells compared to non-ARDS patients. Of interest, comparison of circulating bulk T cells in ARDS patients to non-ARDS patients demonstrated decreased frequencies of CD4$^+$ and CD8$^+$ T cell subsets, with activated memory/effector T cells expressing tissue migration molecule CD11a^{++}. Importantly, survival from ARDS (4/10) was accompanied by a recovery of the CD11a^{++} T cell subsets in peripheral blood. Conclusively, data on S-protein-reactive polyfunctional T cells indicate the ability of ARDS patients to generate antiviral protection. Furthermore, decreased frequencies of activated memory/effector T cells expressing tissue migratory molecule CD11a^{++} observed in circulation of ARDS patients might suggest their involvement in ARDS development and propose the CD11a-based immune signature as a possible prognostic marker.

INTRODUCTION

The SARS-CoV-2 pandemic has confronted the global population with tremendous health, social, and economic challenges. SARS-CoV-2 infections have a broad spectrum of manifestations, ranging from mild to severe symptoms, encompassing pneumonia, acute respiratory distress syndrome (ARDS), and multi-organ failure.[1,2] Usually, a protective role of cellular immunity able to control viral infections is assumed.[3–5] However, an overwhelming immune response after viral infections leading to cell damage and organ failure was also reported.[6] Given that the host immune response to SARS-CoV-2 remains poorly understood, efforts are ongoing to characterize further both cellular and humoral host defense mechanisms. The current lack of knowledge surrounding the SARS-CoV-2 immune response also makes it difficult to interpret COVID-19 disease pathogenesis and potentially impedes vaccine development.

Received 10 July 2020; accepted 30 September 2020;
https://doi.org/10.1016/j.ymthe.2020.10.001.

[11]These authors contributed equally to this work.

Correspondence: Nina Babel, Berlin Institute of Health, Berlin-Brandenburg Center for Regenerative Therapies, and Institute of Medical Immunology, Charité-Universitätsmedizin Berlin, Corporate Member of Freie Universität Berlin, Humboldt-Universität zu Berlin, Augustenburger Platz 1, 13353 Berlin, Germany.
E-mail: nina.babel@charite.de

Table 1. Characteristics of COVID-19 Patients

			Disease Severity		
	Non-COVID-19	Non-COVID-19 Pneumonia	COVID-19 Control	ARDS	p Value
Number of patients	10	3	35 (77.8%)	10 (22.2%)	–
Available follow-up data	n.a.	n.a.	22 (62.9%)	4 (40%)	0.281
Time after PCR diagnosis of initial visit (days)	n.a.	n.a.	2 [1–3]	7 [3–10]	0.015
Time after PCR diagnosis of follow-up visit (days)	n.a.	n.a.	8 [6–15]	31 [29–32]	0.003
Age (years)	55 [51–57]	51 [32–70]	65 [57–81]	58 [48–74]	0.199
Sex (male/female)	5/5 (50.0%/50.0%)	2/1 (66.7%/33.3%)	17/18 (48.6%/51.4%)	10/0 (100.0%/0.0%)	0.003
Comorbidities					
Cancer	0.0 (0.0%)	n.a.	10 (28.6%)	1 (10.0%)	0.409
Chronic renal disease	0.0 (0.0%)	n.a.	6 (17.1%)	0 (0.0%)	0.312
Obstructive lung disease	n.a.	n.a.	3 (8.6%)	0 (0.0%)	1.000
Diabetes	0.0 (0.0%)	n.a.	9 (25.7%)	1 (10.0%)	0.415
Cardiovascular disease	0.0 (0.0%)	n.a.	21 (60.0%)	5 (50.0%)	0.720

The p value refers to the comparison between the ARDS and the COVID-19 control sub-cohorts. Quantitative variables are expressed as median (interquartile range [IQR]) and compared by the Mann-Whitney test. Categorical variables were compared using Fisher's exact test. n.a., not applicable.

Despite the many similarities of the immune response to SARS-CoV-2 and SARS-CoV-1,[7] it is currently not clear whether the disease severity is caused by uncontrolled virus replication, a hyperreactive immune response, or both.[8–10] There is mounting evidence that a cytokine storm with a high level of interleukin (IL)-6 production is associated with severe disease,[2,11,12] suggesting a pathological immune dysregulation. Furthermore, immune paralysis has also been suggested[13] based on single-cell RNA sequencing, demonstrating an increase in $CD4^+$ T cells and a decrease in $CD8^+$ T cells in bronchial lavage samples from clinically well-characterized patients.[14–16] In contrast, markedly lower immune cell numbers and decreased activation levels of specific subsets of T cells have been associated with critical COVID-19 manifestations.[17–19] It has further been observed that a deficiency of Toll-like receptor 7 (TLR7), which is important for pathogen recognition and activation of innate immunity, results in a lack of interferon (IFN)-γ, which may lead to uncontrolled virus replication and ARDS development.[20] There are, however, conflicting data on the association of IFN-γ and COVID-19 severity.[19,21]

Several recent studies have shown that hyperreactive immunity contributes to critical COVID-19 manifestations.[16,18,22–25] One of these studies demonstrated detectable Spike protein-reactive T cell levels in COVID-19 patients with ARDS.[25] However, their role in the development of COVID-19-related ARDS remains unclear. In this study, we performed a comparative analysis of S-protein-reactive T cells collected from ARDS patients and non-ARDS patients to study the contribution of cellular immunity to disease progression. Moreover, we profiled circulating T cells displaying an activated memory phenotype and migratory capacity using multiparametric flow cytometry to explore the T cell migration patterns associated with ARDS development. A detailed characterization of non-specific and SARS-CoV-2-reactive cellular and humoral immunity in a cohort of patients with different disease severity, as well as a healthy cohort, is presented herein. This study may contribute to understanding the immune system's role in COVID-19 progression.

RESULTS

Participant Characteristics and Disease Progression

Forty-five hospitalized patients with mild or moderate COVID-19 disease manifestations (COVID-19 control; n = 35) and COVID-19-associated ARDS (ARDS; n = 10) were enrolled in this study. The patients were analyzed at two time points, that is, shortly after disease onset (initial visit) and after clinical improvement (follow-up visit). For the COVID-19 control group, the initial visit corresponded to hospitalization. For the ARDS group, the initial visit corresponded to the first available visit after ARDS symptoms were observed. The follow-up visit corresponded to the time point of discharge. There were significant differences between the two groups in the times from diagnosis of COVID-19 by PCR to the visits. For ARDS patients, the initial visit and the follow-up visit occurred at a median of 5 days and 23 days later than in the COVID-19 control group. These differences were expected, since the visits correlated to the clinical status of the patients (initial visit, disease onset; follow-up visit, disease resolution). Nevertheless, the effects of the time differences on the results were analyzed in detail and are shown below.

Six of 10 (60.0%) of the ARDS patients succumbed to the infection, while 4 of 10 (40.0%) of the ARDS patients survived and could be transferred from the intensive care unit to regular care about a month after enrollment in the study. All COVID-19 control patients recovered within approximately 2 weeks and were discharged. The detailed characteristics of study patients, study design, blood sampling, and therapy are presented in Tables 1 and S1 and Figure 1. There were no statistically significant differences in age between the analyzed groups. A similar analysis could not be conducted for sex since all ARDS patients were male. Nevertheless, to exclude a potential bias

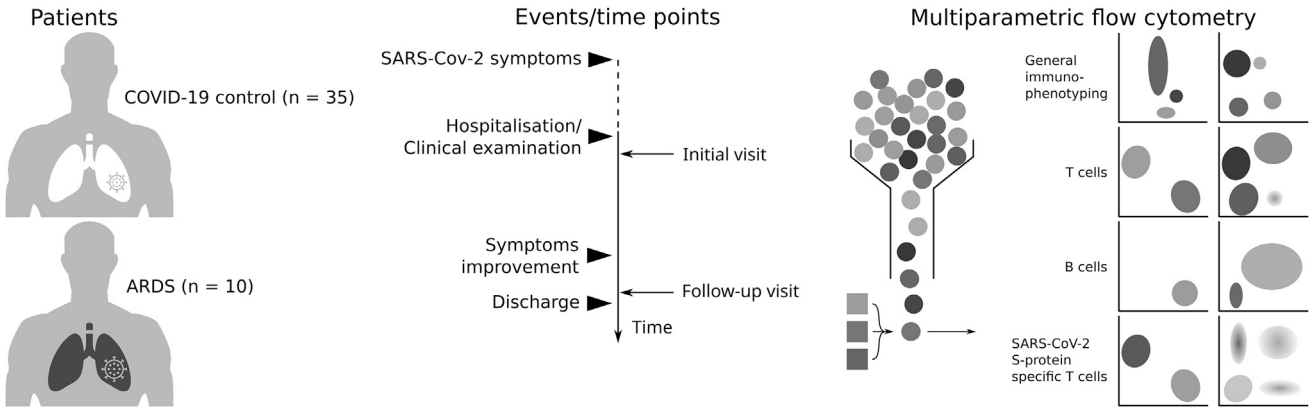

Figure 1. Study Outline

45 patients consecutively admitted to Marienhospital Herne–Universitätsklinikum der Ruhr-Universität Bochum (North Rhine-Westphalia, Germany) and Universitätsklinikum Essen (North Rhine-Westphalia, Germany) were enrolled in this study. The patients were classified based on their symptoms as non-critical COVID-19 course (COVID-19 control) or COVID-19-associated ARDS (ARDS). The patients were analyzed at two time points: shortly after hospitalization (initial visit) and after clinical improvement (follow-up visit). For the ARDS group, the initial visit corresponds to the first available visit after ARDS symptoms were observed, and the follow-up visit corresponds to discharge from the intensive care unit (ICU). The profiling included evaluation of SARS-CoV-2 S-protein-specific IgG serum antibodies, as well as phenotyping of all major immune cell populations by flow cytometry, and characterization of B and T cell subsets. T cells reactive to the SARS-CoV-2 S-protein were also analyzed by application of overlapping peptide pools.

of the results caused by the sex mismatch between the groups, we performed a bivariate regression analysis for all relevant factors (Table S2, and described in more detail in the corresponding parts of Results).

The Degree of Lymphopenia Is Associated with COVID-19 Severity

The absolute counts of circulating leukocytes, including lymphocytes, granulocytes, and monocytes, were below the reference level at the first visit and at the follow-up visit for most patients (Figure S1). At the initial visit, ARDS patients showed significantly lower lymphocyte, $CD3^+$ T cell, and natural killer (NK) cell counts than did the control group. Furthermore, we observed a significantly higher eosinophil count in ARDS patients at the initial visit.

To exclude patient-specific variations caused by lymphopenia, the analysis of the T cell compartments was based on relative values. For the initial visit, the relative frequency of lymphocytes within the leukocyte population was significantly lower in the ARDS group (Figure S1H). At the same time, no significant differences were observed in subtypes of T cells in this group (Figures S1I–S1K). Interestingly, after the improvement of COVID-19 symptoms, the differences in the distribution of the lymphocyte frequency for the COVID-19 control group and ARDS survivors decreased. However, no general conclusion should be made from this observation due to the low number of ARDS survivors. The bivariate regression analysis found no evidence of a confounding effect of sex for the differences in circulating leukocytes between the two groups ($p > 0.05$, Table S2).

Increased Magnitude and Functionality of SARS-CoV-2-Reactive T Cells in ARDS Patients

Next, we analyzed whether ARDS patients were able to generate a SARS-CoV-2-reactive T cell response and how this response differed between the ARDS and COVID-19 control group. At the initial visit, we found more ARDS patients with detectable SARS-CoV-2-reactive $CD4^+CD154^+$ T cells as compared to the control group (10/17 [58.8%] versus 8/10 [80.0%], respectively); however, this difference was not statistically significant (Table S3). The number of patients with detectable S-protein-reactive $CD4^+$ T cells increased to 100.0% at follow-up in both groups (12/12 versus 4/4, respectively) (Table S3). Interestingly, during the whole observation period, a lower percentage of patients in the COVID-19 control group had detectable $CD8^+CD137^+$ T cells (initial visit, 7/17 [41.2%]; follow-up, 5/12 [41.7%]), whereas in the ARDS group, the frequency was comparable to that of $CD4^+CD154^+$ T cells (initial visit, 8/10 [80.0%]; follow-up, 4/4 [100.0%]). However, none of these differences was statistically significant, and caution is advised in the interpretation of these results, due to the low number of ARDS survivors in our study cohort.

Furthermore, we compared the magnitude of T cell responses between the groups. At the initial visit, we found a significantly higher frequency of S-protein-reactive $CD4^+CD154^+$ and $CD8^+CD137^+$ T cells in ARDS patients as compared to controls (Figure 2). The absolute counts of S-protein-reactive T cells showed statistically significant differences only for $CD8^+CD137^+$. $CD4^+CD154^+$ T cells demonstrated a tendency toward a higher number in ARDS patients but did not reach statistical significance, presumably due to general lymphopenia (Figure S2). Looking at $CD4^+$ T cells, we further detected a significant difference in the frequency of $CD4^+CD154^+$ T cells producing IL-2 (Figure 2A). Similar to $CD4^+CD154^+$cells, the data on absolute counts of IL-2-producing $CD4^+CD154^+$ T cells did not reach statistical significance due to lymphopenia (Figure S2A). Although we found significantly higher frequencies and counts for $CD8^+CD137^+$ cells in ARDS patients, the number of

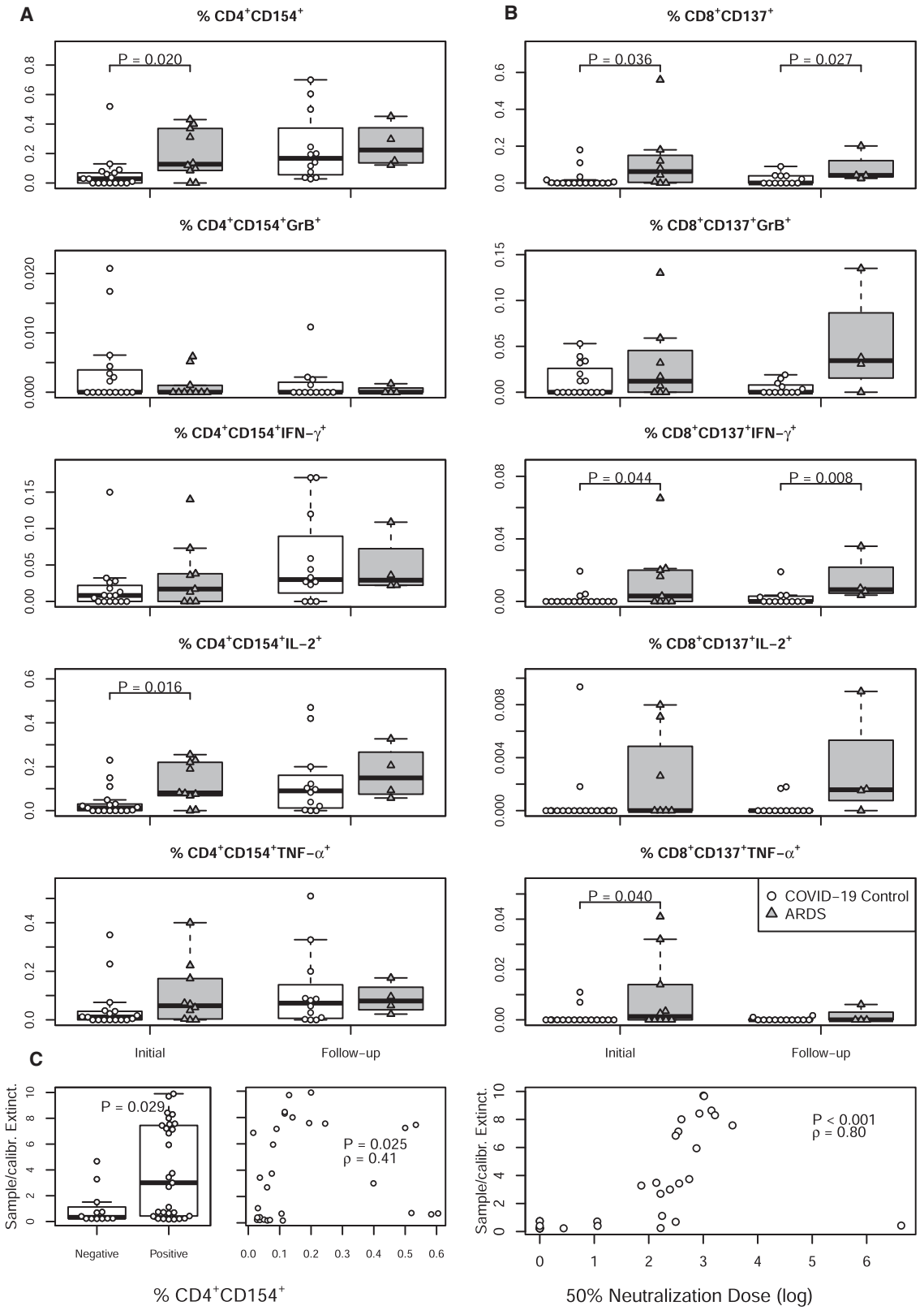

(legend on next page)

S-protein-reactive $CD8^+CD137^+$ T cells was generally very low, and no interpretation of the differences in cytokine-producing $CD8^+CD137^+$ T cells could be achieved. Interestingly, despite the low number of ARDS survivors (4/10), these patients still showed significantly higher $CD8^+CD137^+$ cell counts at the follow-up visit. We found no evidence of a confounding effect of sex for the encountered differences between ARDS patients and COVID-19 controls and in SARS-CoV-2-reactive T cells ($p > 0.05$, Table S2).

Polyfunctional T cells, defined by the expression of more than one cytokine, have been described as a hallmark of protective immunity in viral infections.[26] Thus, we evaluated the combined expression of IL-2, tumor necrosis factor (TNF)-α, IFN-γ, and granzyme B. At both visits the $CD4^+$ T cell response was dominated by double cytokine-producing T cells in ARDS patients and the COVID-19 controls (Table S4). While all ARDS patients demonstrated bi-functional $CD4^+$T cells, only 70%–80% of patients in the COVID-19 control showed double cytokine-producing $CD4^+$ T cells. $CD4^+$ T cells simultaneously producing three or four cytokines were detected in fewer patients for both groups at the initial visit. However, at follow-up, 100% of ARDS patients demonstrated detectable tri-functional $CD4^+$ T cells as compared to only 53% in the control group. A similar prevalence of bi-functional cells was found for $CD8^+$ T cells, with the number of patients with detectable three- and four-functional $CD8^+$ T cells being lower in both groups. However, comparing both groups at the initial and follow-up visits, we observed a significantly higher prevalence of patients with tri-functional $CD8^+$ T cells in ARDS patients, as compared to the COVID-19 controls.

To better evaluate the specificity of the findings on S-protein-reactive T cells in COVID-19 patients, we analyzed S-protein-reactive T cells in blood samples of a small cohort of SARS-CoV-2 unexposed healthy donors (n = 10) and compared them to the COVID-19 control group (Figure S3). While a general tendency for more S-protein-reactive T cells with significant differences for $CD4^+CD154^+$, $CD4^+CD154^+$ $IL\text{-}2^+$, and $CD4^+CD154^+TNFa^+$ was observed in COVID-19 patients, a $CD4^+$ and $CD8^+$ T cell response against the S-protein was also detectable in several SARS-CoV-2 unexposed, healthy donors. As already demonstrated in previous studies,[27,28] these findings might indicate reactivity against common cold corona viruses[29–31] in non-COVID-19 subjects.

Correlation between SARS-CoV-2-Specific Humoral and Cellular Immunity

The activation of B cells by $CD4^+$ T cells is crucial for the induction of a robust antibody response. As expected, we found a correlation between humoral and cellular immunity. Samples with detectable SARS-CoV-2-reactive $CD4^+CD154^+$ T cells had significantly higher antibody titers, independent of the visit time points (Figure 2C). Moreover, among the samples with a detectable anti-SARS-CoV-2 $CD4^+$ response, both frequency and counts of $CD4^+CD154^+$ T cells correlated significantly with the magnitude of the humoral response (Figure S2C). Importantly, we also observed a strong correlation between antibody titers and the 50% neutralization dose (Figure 2C), indicating neutralizing capacity of most of the anti-SARS-CoV-2 antibodies.

ARDS Is Associated with Decreased Frequencies of Lymphocytes with a Differentiated and Activated Cytotoxic Phenotype

Given the observed increased magnitude of antiviral T cell responses in ARDS patients, we further explored the activation/differentiation status of T cells in the peripheral circulation. We evaluated and compared the alteration of various T and B cell subsets between ARDS patients and COVID-19 controls at the initial visit and at follow-up visits (Figure 3). ARDS patients displayed a significantly lower number of central memory $CD4^+$ cells, but not $CD8^+$ cells (Figures 3A and 3B). No significant difference was observed for TEMRA cells. However, a strong trend toward a reduced $CD8^+$ cell count in the ARDS population at the initial visit was observed ($p = 0.08$) (Figures 3C and 3D). We then analyzed the expression of major histocompatibility complex (MHC) class II human leukocyte antigen (HLA)-DR, which is expressed on activated and proliferating T cells, CD57, which is mainly expressed on highly cytotoxic but senescent T cells, and CD28, which is a co-stimulatory molecule and essential for T cell activation, survival, and proliferation.[32–34] We found significantly lower frequencies of T cells with an activated effector phenotype expressing HLA-DR (Figures 3E and 3F) in ARDS patients compared to COVID-19 controls. While no clear effect on $CD57^+$ was observed (Figures 3G and 3H), a significant reduction of $CD28^+CD4^+$ T cells but not $CD28^+CD8^+$ T cells was also observed in ARDS patients (Figures 3I and 3J). Interestingly, we found significantly lower frequencies of CD11a-expressing $CD4^+$ and $CD8^+$ T cells in all ARDS patients (Figures 3K and 3L). In the

Figure 2. Increased Magnitude of Cytokine Producing S-Protein-Reactive T Cells in ARDS Patients in the Initial Visit and at Follow-up

The presence and functional status of SARS-CoV-2-reactive T cells was evaluated using PBMCs, isolated from the peripheral blood of 27 patients (17 COVID-19 control, in white, and 10 ARDS, in gray). Defrosted PBMCs rested for 24 h before treatment with overlapping peptide pools covering immune-dominant regions of the SARS-CoV-2 S-protein. The cells were stimulated for a total of 16 h and in the presence of brefeldin A for the last 14 h. The complete gating strategy is presented in Figure S6. No measurements of IgG antibodies were available for ARDS patients. (A) $CD4^+CD154^+$ frequency (first row) for ARDS and COVID-19 control patients at the initial visit (left boxplots) and follow-up (right boxplots), and frequencies of $CD4^+CD154^+$ cells expressing granzyme B (GrB), INF-γ, IL-2, and TNF-α (rows two to four). (B) $CD8^+CD137^+$ frequency (first row) for ARDS and COVID-19 control patients at the initial visit (left boxplots) and follow-up (right boxplots), and frequencies of $CD8^+CD137^+$ cells expressing GrB, INF-γ, IL-2, and TNF-α (rows two to four). Boxplots depict the median and the first and third quartiles. The whiskers correspond to 1.5 times the interquartile range. (C) Left side: comparison of the relative titers of SARS-CoV-2 S-protein-specific IgG antibodies, measured by ELISA and evaluated as the ratio to an internal control for samples with SARS-CoV-2-specific $CD4^+$ T cells; the comparison of the relative titers classified depending on whether they had detectable virus-specific $CD4^+$ T cells and the correlation of the relative titers with the frequency of virus-specific $CD4^+$ T cells are shown. Right side: comparison of the relative titers of SARS-CoV-2 S-protein-specific IgG antibodies with the 50% neutralization dose. For the analysis of the antibody neutralization dose, the data were log transformed, assigning a value of zero for those with a value below the detection limit.

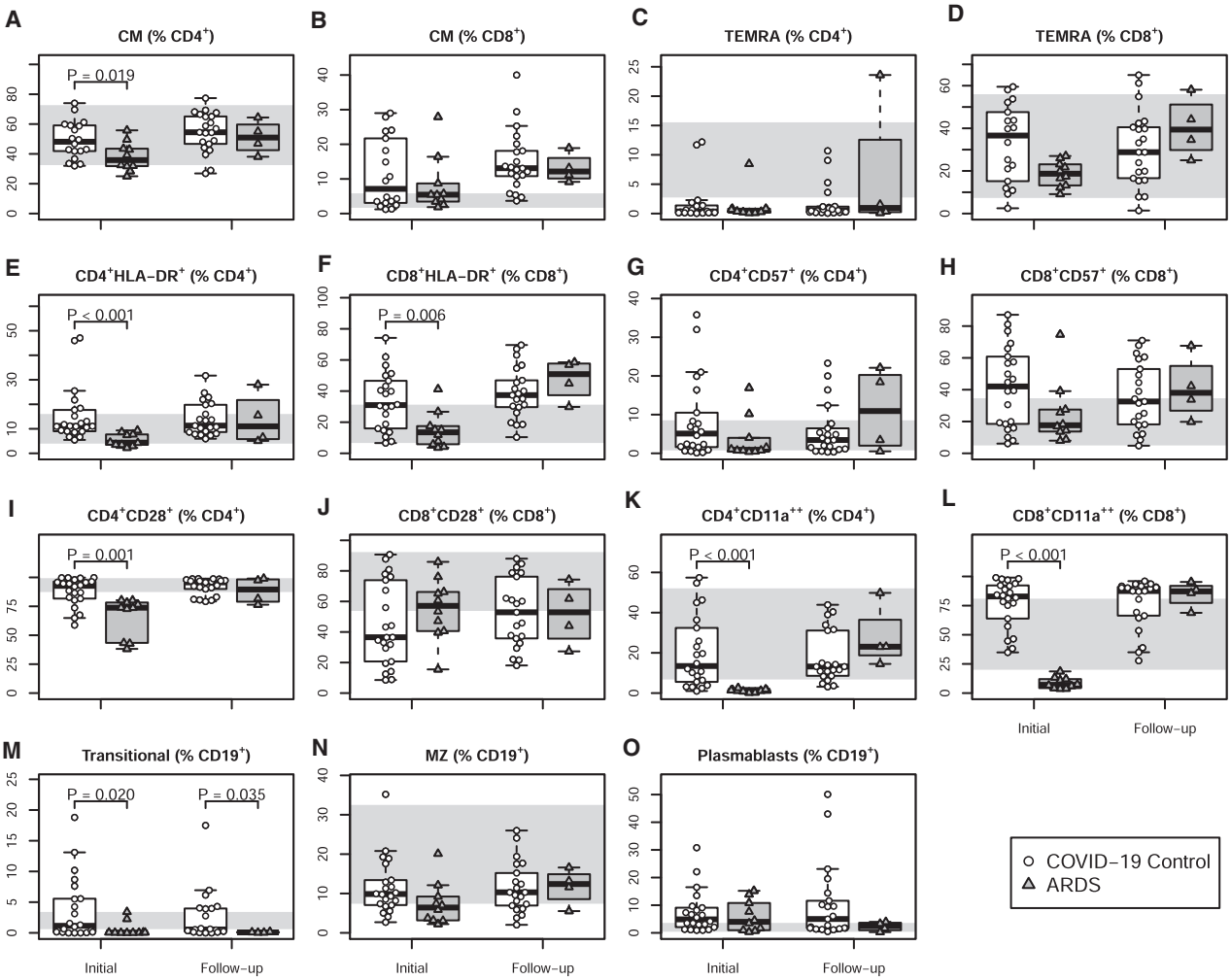

Figure 3. Decrease of Lymphocyte Frequencies with Differentiated and Activated Cytotoxic Phenotype in ARDS Patients at the Initial Visit

Peripheral blood from 37 patients from the COVID-19 control group (n = 27, in white) or ARDS group (n = 10, in gray) was subjected to evaluation for differentiation (A-D) and activation state of T cell (E-L) and B cell (M-O) subsets using multiparametric flow cytometry. The subsets of the $CD3^+$ T cells and the $CD19^+$ B lymphocyte were identified according to the gating strategy depicted in Figures S8–S10. In all cases, the left boxplots show the data for the initial visit, while the right boxplots depict the data at follow-up. The shaded area indicates the reference range as detected in healthy individuals. Boxplots depict the median and the first and third quartiles. The whiskers correspond to 1.5 times the interquartile range.

B cell compartment, we found a significant reduction in the frequencies of transitional $CD19^+$ cells in all ARDS patients (Figure 3M). At the same time, no effect of disease severity was observed on marginal zone B cells or plasmablasts (Figures 3N and 3O). With the improvement of the clinical manifestations at the follow-up visit, the differences between the two groups became less marked, except for the frequencies of transitional $CD19^+$ cells, which remained low for all ARDS patients (Figure 3M).

Overall, we observed a decrease in the frequency of activated and differentiated effector T cells in the peripheral circulation of ARDS patients. We further analyzed the changes in the T cell subsets for the four ARDS survivors (Figure 4). Interestingly, despite the low patient numbers, a significant recovery of the reduced frequencies of $CD11a^{++}$ T cells among $CD4^+$ and $CD8^+$ T cells (Figures 4A and 4B) was observed. We could find a significant increase in $CD8^+CD11a^{++}$ cells expressing HLA-DR, CD28, and CD57 (Figures 4D and 4F). $CD4^+CD11a^{++}$ cells expressing HLA-DR, CD28, and CD57 also increased; however, without reaching statistical significance (Figures 4C, 4E, and 4H). Importantly, a comparison with a small cohort of patients on mechanical ventilation due to non-COVID-19 pneumonia and sepsis seemed to support the hypothesis that the observed alterations were specific for SARS-CoV-2 infection (Figure S4).

In addition, bivariate regression was performed to exclude a possible confounding effect of sex for the identified cellular alterations

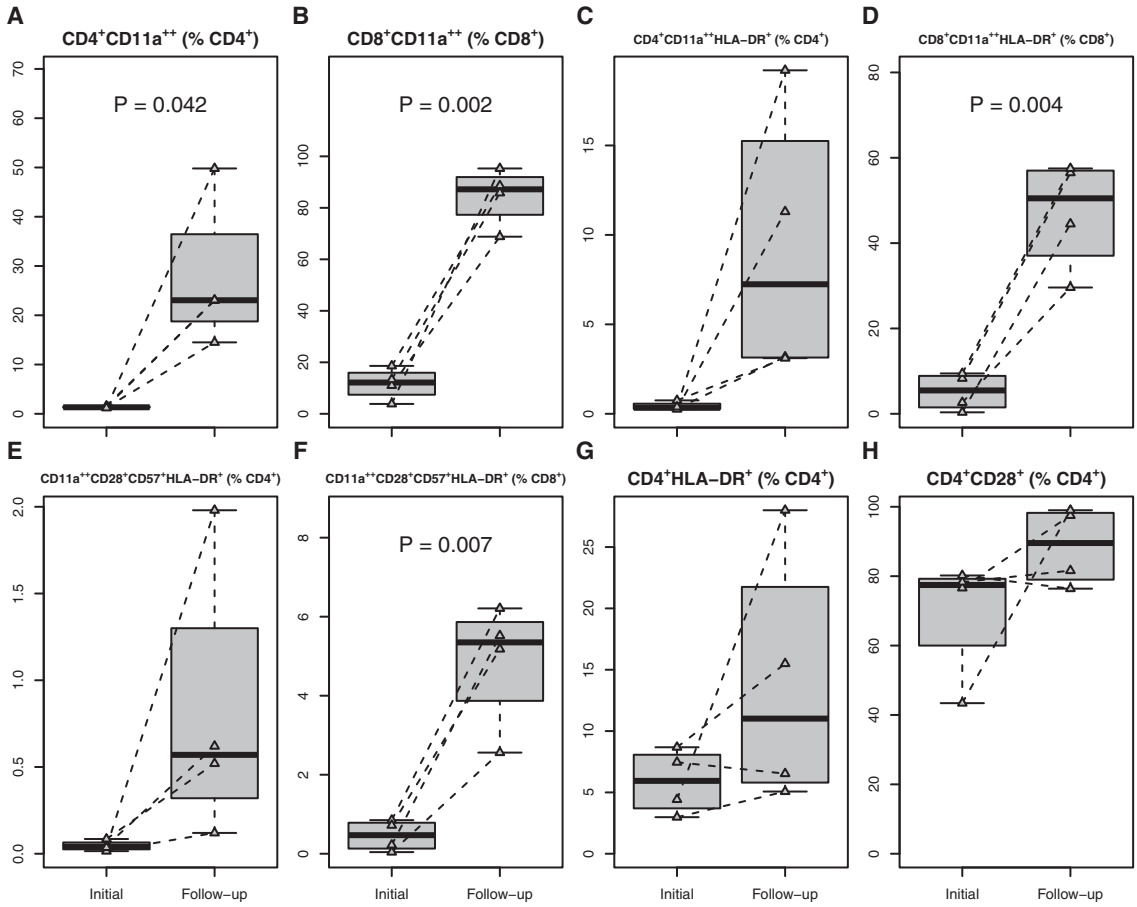

Figure 4. Recovery from ARDS Is Accompanied by the Recovery of Depleted T Cell Subsets with an Activated Differentiated Effector Phenotype

The kinetics of T cell subsets with an activated terminally differentiated effector phenotype were evaluated in the four ARDS survivors. The subsets of the $CD3^+$ T cells were identified according to the gating strategy in Figure S8, and showing cells expressing CD11a (A and B), $CD11a^{++}HLA\text{-}DR^+$ (C and D), $CD11a^{++}CD28^+CD57^+HLA\text{-}DR^+$ (E and F), HLA-DR (G) and CD28 (H). Boxplots depict the median and the first and third quartiles. The whiskers correspond to 1.5 times the interquartile range.

(Table S2). In the present study, a potential confounding sex effect for $CD4^+CD11a^{++}$ was observed. However, this effect can be neglected, since the same ARDS patients showed a very strong recovery for the described subsets at follow-up (Figure S4A). For the other markers significantly associated with COVID-19 ARDS, no significant sex effect was found (Table S2).

Demonstrated Immune Alterations Are Not Due to the Sampling Time Bias

To confirm that the observed results were not due to the differences in follow-up duration, we performed additional analyses using samples of both groups obtained at similar time points in days after initial diagnosis (7 [3–10] days for the COVID-19 controls versus 8 [6–15] days for the ARDS cohort; p = 0.766). The comparison was performed for all markers that showed significant differences at the initial visit (Figure S5). With all of these precautions in place, the differences in leukocyte subsets were still found to be significant, except for the eosinophil counts (Figures S5A–S5E), where the difference detected at the initial visit disappeared with time. While no differences were observed for $CD4^+CD154^+$ cells, an apparent difference remained for $CD8^+CD137^+$ cells (Figures S5F–S5H). Importantly, none of the differentiation and activation markers associated with ARDS showed evidence for a bias of time: for $CD4^+$CM, $CD4^+HLA\text{-}DR^+$, $CD8^+HLA\text{-}DR^+$, $CD4^+CD11a^{++}$, $CD8^+CD11a^{++}$, $CD4^+CD28^+$, and transitional B cells a significant difference was found between the COVID-19 control and the ARDS group at the the matched time points (Figures S5I–S5O).

DISCUSSION

Herein, we present a comprehensive immune profiling study in a cohort of 45 COVID-19 patients, where 35 patients had mild to moderate symptoms, and 10 patients suffered from severe COVID-19-associated ARDS. Our data suggest an intriguing association with the quantitative composition and functionality of several immune cell subsets and the clinical manifestation of COVID-19, pointing to a potential pathogenic immune response in ARDS patients. The

most potent SARS-CoV-2-specific T cell immunity was detected in patients with the worst lung tissue damage, similar to findings described in previous studies.[35] Furthermore, this is a hitherto unreported significant and temporary reduction of circulating $CD11a^{++}$ T cells, suggesting that migration of these cells from the vasculature into the adjacent tissue followed by a specific immune reaction may constitute a pathophysiological mechanism for tissue injury in COVID-19.

Impaired immune regulation and increased inflammation have been reported for patients with SARS-CoV-2-related ARDS.[18,25] Patients with ARDS showed IL-6-driven hyperinflammation and T and B cell lymphopenia.[18] In line with these findings, we found lower numbers of circulating T and B cell subsets in COVID-19-associated ARDS patients compared to mild/moderate COVID-19 control patients. The ARDS group had significantly lower frequencies of T cell subsets with advanced differentiation, activation, and functional properties, which are known to be involved in immune activation and the cytotoxic response against foreign antigens.[36–38] The reason for the reduction in these effector T cells in the circulation of this group of patients is not yet fully understood. It could potentially be caused by activation-induced apoptosis or by inflammation-triggered cell migration.[39] The latter is more plausible given that CD11a is a key T cell integrin, essential for T cell activation and migration.[40] This hypothesis is further supported by the clinical improvement in the four ARDS survivors being accompanied by a normalization of the frequency of $CD11a^{++}$ T cells in the peripheral blood.

Although the information is sparse, several groups have reported on lung-infiltrating T cells in COVID-19 patients to a more considerable degree than observed for influenza infection.[41,42] An increase in $CD4^+$ T cells and a decrease in $CD8^+$ T cells in patients with severe manifestations have been identified using single-cell RNA sequencing of bronchoalveolar lavage from COVID-19 patients.[14,43] Furthermore, a negative association between IL-6 serum levels, a cytokine known to upregulate the expression of the migratory chemokine receptors CXCR6 and CCR5 on memory T cells,[44] and the number of T cells in the circulation has been observed.[45,46] There are also reports showing increased expression of CXCR6 on lung T cells, as compared to peripheral blood T cells.[47,48] As such, we deem it a likely hypothesis that lymphocyte migration into tissues, triggered by inflammation, may be responsible for the reduction of activated terminally differentiated T cell subsets in the peripheral blood. This hyposthesis should be tested in future studies, keeping in mind that lungs might not be the only target for the migrating T cells, as extrapulmonary manifestations of COVID-19 have been reported.[49–53]

Our findings support the proposed hypothesis of immunopathogenesis as a leading cause of COVID-19 severe morbidity and mortality.[10,54–56] In the studied patients, we observed an increased frequency of SARS-CoV-2 S-protein-reactive $CD4^+$ and $CD8^+$ T cells in the ARDS group. The antiviral activity of the detected T cells could be confirmed by their polyfunctionality as defined by the simultaneous release/expression of several cytokines.[26] The magnitude of the S-protein-reactive T cell response is also comparable with earlier data reported on S-protein-reactive T cells in patients with COVID-19-associated ARDS.[25] The reason for the observed higher number of SARS-CoV-2-reactive T cells in ARDS patients might potentially be explained by a disturbed migration of antigen-specific cells into the infected tissue, leading to impaired viral clearance. Another explanation is the unspecific migration of effector T cells into this area through bystander activation, leading to increased inflammation within infected tissue and the relative abundance of S-protein-reactive T cells in the circulation. Therefore, the evaluation of S-protein-reactive T cells expressing the tissue homing marker CD11a may be an important prognostic tool to understand the migratory behavior of antiviral T cells and should be performed in future studies. However, it is also possible that the composition of the peripheral immune cells mirrors the situation in the infected tissue, where severe virus infection with high antigen load led to generation of the large number of antigen-reactive effector T cells, causing injury of the affected organ.

Although the protective capacity of SARS-CoV-2-reactive T cells still needs to be evaluated, COVID-19 disease progression was accompanied by a higher magnitude of IL-2-, IFN-γ- and TNF-α-producing cells. This finding has important clinical implications in terms of the potential therapeutic effects of immunosuppressive approaches at this stage of the disease. Indeed, recent studies described a positive effect of anti-IL-6 or anti-IL-1 therapy, with similar observations reported in the Randomized Evaluation of COVID-19 Therapy (RECOVERY) study (ClinicalTrials.gov: NCT04381936) for dexamethasone in ARDS patients.[18,24,55,57,58]

In conclusion, the data presented herein are supportive of immune pathogenesis as an underlying cause of COVID-19-associated ARDS. Additionally, the identified CD11a-based immune signature could be used as a novel prognostic marker for disease progression. Since most immunodiagnostic laboratories already offer the proposed marker analysis, multi-center evaluation of this marker should be contemplated, so it can readily be utilized for patient monitoring in the current pandemic.

MATERIALS AND METHODS

Study Population and Design

Forty-five patients with a mild and moderate COVID-19 course (COVID-19 control, n = 35) or COVID-19-associated ARDS (ARDS; n = 10) consecutively admitted to University Hospitals Essen and Bochum, Germany, were recruited into the study. The classification of COVID-19 manifestation was performed following Siddiqi and Mehra.[1] Subjects were eligible for enrollment when they met the following inclusion criteria: (1) a positive SARS-CoV2 PCR test and (2) signed written informed consent. The patients of the COVID-19 control group were recruited after COVID-19 diagnosis (initial visit). For ARDS patients, recruitment took place at the first available time point after ARDS diagnosis. The second sample was

available after clinical improvement at patient discharge (follow-up visit). A small cohort of patients with non-COVID-19 pneumonia requiring mechanical ventilation (n = 3) and SARS-CoV-2 unexposed healthy donors (n = 10) recruited before COVID-19 pandemics were also included as controls.

Demographics and clinical characteristics of patients are shown in Tables 1 and S1.

Preparation of PBMCs

Peripheral blood was collected in S-Monovette K3 EDTA blood collection tubes (Sarstedt). Collected blood was pre-diluted in PBS/BSA (Gibco) at a 1:1 ratio and underlaid with 15 mL of Ficoll-Paque Plus (GE Healthcare). Tubes were centrifuged at 800 × *g* for 20 min at room temperature. Isolated peripheral blood mononuclear cells (PBMCs) were washed twice with PBS/BSA and stored at −80°C until use as previously described.[59]

Stimulation with SARS-CoV-2 Overlapping Peptide Pools

Isolated PBMCs were stimulated with SARS-CoV-2 PepTivator (Miltenyi Biotec) overlapping peptide pools (OPPs) containing overlapping peptides spanning the immune dominant regions of surface glycoprotein as predicted by *in silico* analysis.[60] The peptide pools (GenBank: MN908947.3, QHD43416.1) include the sequence domains amino acids 304–338, 421–475, 492–519, 683–707, 741–770, 785–802, and 885–1273. Peptide pools were dissolved per the manufacturer's directions and used at a concentration of 1 μg/mL. 2.5×10^6 PBMCs were thawed and plated for each condition in 96-U-Well plates in RPMI 1640 media (Life Technologies), supplemented with 1% penicillin-streptomycin-glutamine (Sigma-Aldrich), and 10% fetal calf serum (FCS) (PAN-Biotech) and were stimulated or left untreated as a control for 16 h. As a positive control, cells were stimulated with staphylococcal enterotoxin B (SEB) (1 μg/mL, Sigma-Aldrich), and negative control was with vehicle (a medium to dissolve peptide pools). After 2 h, brefeldin A (1 μg/mL, Sigma-Aldrich) was added. As previously applied by our groups and others, antigen-specific responses were considered positive after the non-specific background was subtracted, and more than 0.001% or at least 15 positive cells were detectable.[5,61] Negative values were set to zero.

Antibodies

Antibodies for general phenotyping were as follows (all antibodies were from BioLegend unless otherwise noted): CD45-Alexa Fluor 488 (A488), clone 2D1; CD56-peridinin chlorophyll protein (PerCP)-Cy5.5, clone NCAM; CD14-phycoerythrin (PE)-Vio 770, clone TÜK4 (Miltenyi Biotec); CD4-Alexa Fluor 700 (A700), clone OKT4; CD16-allophycocyanin (APC)-Vio 770, clone REA423 (Miltenyi Biotec); CD8-V500, clone RPA-T8 (Becton Dickinson); CD19-Brilliant Violet 605 (BV605), clone HIB19; HLA-DR-Brilliant Violet 650 (BV650), clone L243; CD3-Brilliant Violet 785 (BV785), clone OKT3.

Antibodies for T cell subsets were as follows (all antibodies were from Beckman Coulter unless otherwise noted): CCR7-PE, clone G043H7; CD127-PC7, clone R34.34; CD25-fluorescein isothiocyanate (FITC), clone B1.49.9; CD3-APC-750, clone UCHT1; CD45RA-Pacific Blue, clone 2H4; CD4-ECD, clone SCF4I12T4D11; CD8-APC, clone B9.11; T cell receptor (TCR)α/β-PerCP-Cy5.5, clone IP26 (BioLegend); TCRγ/δ-Brilliant Violet 510 (BV510), clone B1 (BioLegend).

Antibodies for the T cell activation state *ex vivo* were as follows (all antibodies were from Beckman Coulter): CD11a-FITC, clone 25.3; CD28- PerCP-Cy5.5, clone CD28.2; CD57-Pacific Blue, clone NC1; CD3-APC-750, clone UCHT1; HLA-DR-PE, clone Immu-357; CD4-ECD, clone SCF4I12T4D11; CD8-APC, clone B9.11.

Antibodies for B cell subsets were as follows (all antibodies were from Beckman Coulter unless otherwise noted): CD19-ECD, clone J3-119; CD21-APC, clone B-ly4 (BD Biosciences); CD24-PerCP-Cy5.5, clone ALB9; CD27-PC7, clone 1A4CD27; CD38-APC-750, clone LS198-4-3; CD45-KrOrange, clone J33; HLA-DR-PE, clone Immu357; immunoglobulin (Ig)D-FITC, clone IA6-2; IgM-Pacific Blue, clone. SA-DA4.

Antibodies for SARS-Cov-2-specific T cells were as follows (all antibodies were from BioLegend unless otherwise noted): surface staining: CCR7 (CD197)-PerCP-Cy5.5, clone G043H7; CD4-A700, clone OKT4; LD eFluor 780 (eBioscience), CD8-V500, clone RPA-T8 (BD Biosciences); CD45RA-BV605, clone HI100. Intracellular staining: granzyme B-FITC, clone GB11; IL-2-PE, clone MQ1-17H12; IL-4-PE-Dazzle 594, clone MP4-25D2; CD137 (4-1BB)-PE-Cy7, clone 4B4-1; CD154 (CD40L)-Alexa Fluor 647 (A647), clone 24-31; TNF-α-eFluor 450, clone MAb11 (eBioscience); IFN-γ-BV650, clone 4S.B3; CD3-Brilliant Violet 785 (BV785), clone OKT3. Fixable viability dye eFluor 780 (eBioscience) was used for live/dead discrimination.

Flow Cytometry

EDTA-treated whole blood was stained with optimal concentrations of each antibody for 10 min at room temperature in the dark. Erythrocytes were lysed using VersaLyse (Beckman Coulter) with 2.5% IOTest 3 fixative solution (Beckman Coulter) for 30 min at room temperature in the dark. Samples for general phenotyping were immediately acquired, while samples for T and B cell subsets were washed twice with PBS/BSA. Samples for the B cell subset were washed twice with PBS prior to staining with antibodies.

T cells stimulated with SARS-Cov-2 OPPs were stained with optimal concentrations of antibodies for 10 min at room temperature in the dark. Stained cells were washed twice with PBS/BSA before preparation for intracellular staining using the Intracellular Fixation & Permeabilization Buffer Set (Thermo Fisher Scientific) as per the manufacturer's instructions. Fixed and permeabilized cells were stained for 30 min at room temperature in the dark with an optimal dilution of antibodies against the intracellular antigen.

All samples were immediately acquired on a CytoFLEX flow cytometer (Beckman Coulter). Quality control was performed daily using

the recommended CytoFLEX daily QC fluorospheres (Beckman Coulter). No modification to the compensation matrices was required throughout the study.

SARS-CoV-2 IgG Antibody Titers

Peripheral blood was collected in S-Monovette Z-Gel (Sarstedt). SARS-CoV-2 IgG titers were analyzed in purified serum using a SARS-CoV-2 IgG kit (Euroimmun, Lübeck, Germany). The test was performed according to the manufacturer's instructions. Briefly, serum samples were diluted 1:100 and added to plates coated with recombinant SARS-CoV-2 antigen. Bound SARS-Cov-2 S1 protein-specific IgG was detected by a horseradish peroxidase (HRP)-conjugated anti-human IgG. The absorbance was read on a microplate reader at 450 nm with reference at 620 nm and evaluated as the ratio the absorbance of the sample to the absorbance of the internal standard.

SARS-CoV-2 Neutralizing Antibodies

To determine the capacity of serum antibodies to neutralize the virus, a propagation-incompetent vesicular stomatitis virus (VSV)*DG (firefly luciferase) pseudovirus system bearing the SARS-CoV-2 spike protein in the envelope was used. The pseudovirus system was incubated with serial dilutions of sera prior to the infection of Vero E6 cells using pseudovirus. Vero E6 cells were maintained in Dulbecco's minimal essential medium (Life Technologies, Zug, Switzerland) supplemented with 10% fetal bovine serum and non-essential amino acids (Life Technologies). 18 h after infection, firefly luciferase reporter activity was determined. The 50% neutralization dose was determined as the reciprocal antibody dilution causing 50% inhibition of the calculated luciferase reporter.

Statistical Analysis

Flow cytometry data were analyzed using FlowJo version 10.6.2 (BD Biosciences); gating strategies are presented in Figures S6–S10. For the analysis of anti-SARS-CoV-2 T cells, a threshold of 0.001% was employed to define a detectable response. For the analysis of the antibody neutralization dose, the data were log-transformed, assigning a value of zero for those with a value below the detection limit. In this study, extremely high values were excluded from analysis; these were determined based on Tukey's fences (k = 3), estimated for all values with a detectable response.

Statistical analysis was performed using R,[62] version 3.6.2. Categorical variables are summarized as numbers and frequencies; quantitative variables are reported as median and interquartile range. Boxplots depict the median and the first and third quartiles. The whiskers correspond to 1.5 times the interquartile range. All applied statistical tests are two-sided. Unless otherwise stated, differences between groups for categorical variables were calculated using Fisher's exact test. Differences in quantitative variables between groups were analyzed using the Mann-Whitney U test. The dynamics of quantitative variables were analyzed using the paired t test, assuming a normal distribution for the differences between the initial and follow-up visit. Correlation size and significance were calculated using Spearman's correlation coefficient. Bivariate regression analysis was performed to exclude potential bias in the analysis due to the unbalanced distribution of the biological sex within the groups. Thus, for factors significantly associated with illness severity, regression analysis was performed with sex and COVID-19 severity as independent variables, without interactions. p values below 0.050 were considered significant; only significant p values are reported in the figures. p values were not corrected for multiple testing, as this study was of an exploratory nature.[63]

Study Approval

The study was approved by the Ethics Committee of the Ruhr University Bochum (20-6886) and University Hospital Essen (20-9214-BO). Written informed consent was obtained from all participants.

SUPPLEMENTAL INFORMATION

Supplemental Information can be found online at https://doi.org/10.1016/j.ymthe.2020.10.001.

AUTHOR CONTRIBUTIONS

Conceptualization, M. Anft, U.S., and N.B.; Data Curation, K.P.; Formal Analysis, M. Anft, A.B.-N., C.J.T., T.R., and U.S.; Funding Acquisition, T.H.W., O.W. and N.B.; Investigation, S.S., E.K., J.K., J.Z., P.W., S.K., and S.B.; Methodology, M. Anft, K.P., C.J.T. and T.R.; Project Administration, U.S. and N.B.; Resources, K.P., A.D., F.S.S., B.H., M. Abou-El-Enein, M.J.K., M.M.B, T.B., C.T., C.W., S.D., U.D., T.H.W., and O.W.; Supervision, T.R., U.S., and N.B.; Visualization, A.B.-N.; Writing – Original Draft, M. Anft, K.P., A.B.-N., C.J.T., T.R., C.W., S.D., U.D., T.H.W., M. Abou-El-Enein, O.W., U.S., and N.B.; Writing – Review & Editing, U.S., M. Anft, A.B.-N., M. Abou-El-Enein, and N.B.

CONFLICTS OF INTEREST

The authors declare no competing interests.

ACKNOWLEDGMENTS

We want to express our deepest gratitude to the patients who donated their blood samples and clinical data for this project. This work was supported by grants from the Mercator Foundation, Germany (St-2018-0014), BMBF e:KID (01ZX1612A), BMBF NoChro (FKZ 13GW0338B), and SepsisDataNet (EFRE-0800984).

REFERENCES

1. Siddiqi, H.K., and Mehra, M.R. (2020). COVID-19 illness in native and immunosuppressed states: a clinical-therapeutic staging proposal. J. Heart Lung Transplant. *39*, 405–407.

2. Guan, W.J., Ni, Z.Y., Hu, Y., Liang, W.H., Ou, C.Q., He, J.X., Liu, L., Shan, H., Lei, C.L., Hui, D.S.C., et al.; China Medical Treatment Expert Group for Covid-19 (2020). Clinical characteristics of coronavirus disease 2019 in China. N. Engl. J. Med. *382*, 1708–1720.

3. Kern, F., Bunde, T., Faulhaber, N., Kiecker, F., Khatamzas, E., Rudawski, I.M., Pruss, A., Gratama, J.W., Volkmer-Engert, R., Ewert, R., et al. (2002). Cytomegalovirus (CMV) phosphoprotein 65 makes a large contribution to shaping the T cell repertoire in CMV-exposed individuals. J. Infect. Dis. *185*, 1709–1716.

4. Stervbo, U., Nienen, M., Weist, B.J.D., Kuchenbecker, L., Hecht, J., Wehler, P., Westhoff, T.H., Reinke, P., and Babel, N. (2019). BKV clearance time correlates

with exhaustion state and T-cell receptor repertoire shape of BKV-specific T-cells in renal transplant patients. Front. Immunol. *10*, 767.

5. Weist, B.J.D., Wehler, P., El Ahmad, L., Schmueck-Henneresse, M., Millward, J.M., Nienen, M., Neumann, A.U., Reinke, P., and Babel, N. (2015). A revised strategy for monitoring BKV-specific cellular immunity in kidney transplant patients. Kidney Int. *88*, 1293–1303.
6. Babel, N., Volk, H.-D., and Reinke, P. (2011). BK polyomavirus infection and nephropathy: the virus-immune system interplay. Nat. Rev. Nephrol. *7*, 399–406.
7. Chen, J., and Subbarao, K. (2007). The immunobiology of SARS. Annu. Rev. Immunol. *25*, 443–472.
8. Moore, J.B., and June, C.H. (2020). Cytokine release syndrome in severe COVID-19. Science *368*, 473–474.
9. Shi, Y., Wang, Y., Shao, C., Huang, J., Gan, J., Huang, X., Bucci, E., Piacentini, M., Ippolito, G., and Melino, G. (2020). COVID-19 infection: the perspectives on immune responses. Cell Death Differ. *27*, 1451–1454.
10. Vabret, N., Britton, G.J., Gruber, C., Hegde, S., Kim, J., Kuksin, M., Levantovsky, R., Malle, L., Moreira, A., Park, M.D., et al.; Sinai Immunology Review Project (2020). Immunology of COVID-19: current state of the science. Immunity *52*, 910–941.
11. Mehta, P., McAuley, D.F., Brown, M., Sanchez, E., Tattersall, R.S., and Manson, J.J.; HLH Across Speciality Collaboration, UK (2020). COVID-19: consider cytokine storm syndromes and immunosuppression. Lancet *395*, 1033–1034.
12. Huang, C., Wang, Y., Li, X., Ren, L., Zhao, J., Hu, Y., Zhang, L., Fan, G., Xu, J., Gu, X., et al. (2020). Clinical features of patients infected with 2019 novel coronavirus in Wuhan, China. Lancet *395*, 497–506.
13. Arunachalam, P.S., Wimmers, F., Mok, C.K.P., Perera, R.A.P.M., Scott, M., Hagan, T., Sigal, N., Feng, Y., Bristow, L., Tak-Yin Tsang, O., et al. (2020). Systems biological assessment of immunity to mild versus severe COVID-19 infection in humans. Science *369*, 1210–1220.
14. Liao, M., Liu, Y., Yuan, J., Wen, Y., Xu, G., Zhao, J., Cheng, L., Li, J., Wang, X., Wang, F., et al. (2020). Single-cell landscape of bronchoalveolar immune cells in patients with COVID-19. Nat. Med. *26*, 842–844.
15. Chua, R.L., Lukassen, S., Trump, S., Hennig, B.P., Wendisch, D., Pott, F., Debnath, O., Thürmann, L., Kurth, F., Völker, M.T., et al. (2020). COVID-19 severity correlates with airway epithelium-immune cell interactions identified by single-cell analysis. Nat. Biotechnol. *38*, 970–979.
16. Guo, C., Li, B., Ma, H., Wang, X., Cai, P., Yu, Q., Zhu, L., Jin, L., Jiang, C., Fang, J., et al. (2020). Single-cell analysis of two severe COVID-19 patients reveals a monocyte-associated and tocilizumab-responding cytokine storm. Nat. Commun. *11*, 3924.
17. Wilk, A.J., Rustagi, A., Zhao, N.Q., Roque, J., Martínez-Colón, G.J., McKechnie, J.L., Ivison, G.T., Ranganath, T., Vergara, R., Hollis, T., et al. (2020). A single-cell atlas of the peripheral immune response in patients with severe COVID-19. Nat. Med. *26*, 1070–1076.
18. Giamarellos-Bourboulis, E.J., Netea, M.G., Rovina, N., Akinosoglou, K., Antoniadou, A., Antonakos, N., Damoraki, G., Gkavogianni, T., Adami, M.E., Katsaounou, P., et al. (2020). Complex immune dysregulation in COVID-19 patients with severe respiratory failure. Cell Host Microbe *27*, 992–1000.e3.
19. Chen, G., Wu, D., Guo, W., Cao, Y., Huang, D., Wang, H., Wang, T., Zhang, X., Chen, H., Yu, H., et al. (2020). Clinical and immunological features of severe and moderate coronavirus disease 2019. J. Clin. Invest. *130*, 2620–2629.
20. van der Made, C.I., Simons, A., Schuurs-Hoeijmakers, J., van den Heuvel, G., Mantere, T., Kersten, S., van Deuren, R.C., Steehouwer, M., van Reijmersdal, S.V., Jaeger, M., et al. (2020). Presence of genetic variants among young men with severe COVID-19. JAMA *324*, 1–11.
21. Mudd, P.A., Crawford, J.C., Turner, J.S., Souquette, A., Reynolds, D., Bender, D., Bosanquet, J.P., Anand, N.J., Striker, D.A., Martin, R.S., et al. (2020). Targeted immunosuppression distinguishes COVID-19 from influenza in moderate and severe disease. medRxiv. https://doi.org/10.1101/2020.05.28.20115667.
22. Lopes, M.I.F., Bonjorno, L.P., Giannini, M.C., Amaral, N.B., Benatti, M.N., Rezek, U.C., Emrich-Filho, L.L., Sousa, B.A.A., Almeida, S.C.L., Luppino-Assad, R., et al. (2020). Beneficial effects of colchicine for moderate to severe COVID-19: an interim analysis of a randomized, double-blinded, placebo controlled clinical trial. medRxiv. https://doi.org/10.1101/2020.08.06.20169573.
23. Beigel, J.H., Tomashek, K.M., Dodd, L.E., Mehta, A.K., Zingman, B.S., Kalil, A.C., Hohmann, E., Chu, H.Y., Luetkemeyer, A., Kline, S., et al.; ACTT-1 Study Group Members (2020). Remdesivir for the treatment of Covid-19—preliminary report. N. Engl. J. Med. Published online May 22, 2020. https://doi.org/10.1056/NEJMoa2007764.
24. Horby, P., Lim, W.S., Emberson, J.R., Mafham, M., Bell, J.L., Linsell, L., Staplin, N., Brightling, C., Ustianowski, A., Elmahi, E., et al.; RECOVERY Collaborative Group (2020). Dexamethasone in hospitalized patients with Covid-19—preliminary report. N. Engl. J. Med. Published online July 17, 2020. https://doi.org/10.1056/NEJMoa2021436.
25. Weiskopf, D., Schmitz, K.S., Raadsen, M.P., Grifoni, A., Okba, N.M.A., Endeman, H., van den Akker, J.P.C., Molenkamp, R., Koopmans, M.P.G., van Gorp, E.C.M., et al. (2020). Phenotype and kinetics of SARS-CoV-2-specific T cells in COVID-19 patients with acute respiratory distress syndrome. Sci. Immunol *5*, eabd2071.
26. Harari, A., Vallelian, F., Meylan, P.R., and Pantaleo, G. (2005). Functional heterogeneity of memory CD4 T cell responses in different conditions of antigen exposure and persistence. J. Immunol. *174*, 1037–1045.
27. Braun, J., Loyal, L., Frentsch, M., Wendisch, D., Georg, P., Kurth, F., Hippenstiel, S., Dingeldey, M., Kruse, B., Fauchere, F., et al. (2020). SARS-CoV-2-reactive T cells in healthy donors and patients with COVID-19. Nature. Published online July 29, 2020. https://doi.org/10.1038/s41586-020-2598-9.
28. Grifoni, A., Weiskopf, D., Ramirez, S.I., Mateus, J., Dan, J.M., Moderbacher, C.R., Rawlings, S.A., Sutherland, A., Premkumar, L., Jadi, R.S., et al. (2020). Targets of T cell responses to SARS-CoV-2 coronavirus in humans with COVID-19 disease and unexposed individuals. Cell *181*, 1489–1501.e15.
29. Mateus, J., Grifoni, A., Tarke, A., Sidney, J., Ramirez, S.I., Dan, J.M., Burger, Z.C., Rawlings, S.A., Smith, D.M., Phillips, E., et al. (2020). Selective and cross-reactive SARS-CoV-2 T cell epitopes in unexposed humans. Science *370*, 89–94.
30. Le Bert, N., Tan, A.T., Kunasegaran, K., Tham, C.Y.L., Hafezi, M., Chia, A., Chng, M.H.Y., Lin, M., Tan, N., Linster, M., et al. (2020). SARS-CoV-2-specific T cell immunity in cases of COVID-19 and SARS, and uninfected controls. Nature *584*, 457–462.
31. Stervbo, U., Rahmann, S., Roch, T., Westhof, T.H., and Babel, N. (2020). SARS-CoV-2 reactive T cells in uninfected individuals are likely expanded by beta-coronaviruses. bioRxiv. https://doi.org/10.1101/2020.07.01.182741.
32. Boomer, J.S., and Green, J.M. (2010). An enigmatic tail of CD28 signaling. Cold Spring Harb. Perspect. Biol. *2*, a002436.
33. Kared, H., Martelli, S., Ng, T.P., Pender, S.L.F., and Larbi, A. (2016). CD57 in human natural killer cells and T-lymphocytes. Cancer Immunol. Immunother. CII *65*, 441–452.
34. Caruso, A., Licenziati, S., Corulli, M., Canaris, A.D., De Francesco, M.A., Fiorentini, S., Peroni, L., Fallacara, F., Dima, F., Balsari, A., and Turano, A. (1997). Flow cytometric analysis of activation markers on stimulated T cells and their correlation with cell proliferation. Cytometry *27*, 71–76.
35. Mathew, D., Giles, J.R., Baxter, A.E., Oldridge, D.A., Greenplate, A.R., Wu, J.E., Oldridge, D.A., Kuri-Cervantes, L., Betina Pampena, M.B., D'Andrea, K., et al. (2020). Deep immune profiling of COVID-19 patients reveals distinct immunotypes with therapeutic implications. bioRxiv. https://doi.org/10.1126/science.abc8511.
36. Chandele, A., Sewatanon, J., Gunisetty, S., Singla, M., Onlamoon, N., Akondy, R.S., Kissick, H.T., Nayak, K., Reddy, E.S., Kalam, H., et al. (2016). Characterization of human CD8 T cell responses in dengue virus-infected patients from India. J. Virol *90*, 11259–11278.
37. Strioga, M., Pasukoniene, V., and Characiejus, D. (2011). $CD8^+$ $CD28^-$ and $CD8^+$ $CD57^+$ T cells and their role in health and disease. Immunology *134*, 17–32.
38. Le Priol, Y., Puthier, D., Lécureuil, C., Combadière, C., Debré, P., Nguyen, C., and Combadière, B. (2006). High cytotoxic and specific migratory potencies of senescent $CD8^+CD57^+$ cells in HIV-infected and uninfected individuals. J. Immunol. *177*, 5145–5154.
39. Zhang, J.-Y., Wang, X.-M., Xing, X., Xu, Z., Zhang, C., Song, J.-W., Fan, X., Xia, P., Fu, J.L., Wang, S.Y., et al. (2020). Single-cell landscape of immunological responses in patients with COVID-19. Nat. Immunol. *21*, 1107–1118.
40. Walling, B.L., and Kim, M. (2018). LFA-1 in T cell migration and differentiation. Front. Immunol. *9*, 952.

41. Xu, Z., Shi, L., Wang, Y., Zhang, J., Huang, L., Zhang, C., Liu, S., Zhao, P., Liu, H., Zhu, L., et al. (2020). Pathological findings of COVID-19 associated with acute respiratory distress syndrome. Lancet Respir. Med. *8*, 420–422.

42. Ackermann, M., Verleden, S.E., Kuehnel, M., Haverich, A., Welte, T., Laenger, F., Vanstapel, A., Werlein, C., Stark, H., Tzankov, A., et al. (2020). Pulmonary vascular endothelialitis, thrombosis, and angiogenesis in Covid-19. N. Engl. J. Med. *383*, 120–128.

43. Bost, P., Giladi, A., Liu, Y., Bendjelal, Y., Xu, G., David, E., Blecher-Gonen, R., Cohen, M., Medaglia, C., Li, H., et al. (2020). Host-viral infection maps reveal signatures of severe COVID-19 patients. Cell *181*, 1475–1488.e12.

44. Hundhausen, C., Roth, A., Whalen, E., Chen, J., Schneider, A., Long, S.A., Wei, S., Rawlings, R., Kinsman, M., Evanko, S.P., et al. (2016). Enhanced T cell responses to IL-6 in type 1 diabetes are associated with early clinical disease and increased IL-6 receptor expression. Sci. Transl. Med *8*, 356ra119.

45. Diao, B., Wang, C., Tan, Y., Chen, X., Liu, Y., Ning, L., Chen, L., Li, M., Liu, Y., Wang, G., et al. (2020). Reduction and functional exhaustion of T cells in patients with coronavirus disease 2019 (COVID-19). Front. Immunol. *11*, 827.

46. Liu, J., Li, S., Liu, J., Liang, B., Wang, X., Wang, H., Li, W., Tong, Q., Yi, J., Zhao, L., et al. (2020). Longitudinal characteristics of lymphocyte responses and cytokine profiles in the peripheral blood of SARS-CoV-2 infected patients. EBioMedicine *55*, 102763.

47. Freeman, C.M., Curtis, J.L., and Chensue, S.W. (2007). CC chemokine receptor 5 and CXC chemokine receptor 6 expression by lung $CD8^+$ cells correlates with chronic obstructive pulmonary disease severity. Am. J. Pathol. *171*, 767–776.

48. Morgan, A.J., Guillen, C., Symon, F.A., Huynh, T.T., Berry, M.A., Entwisle, J.J., Briskin, M., Pavord, I.D., and Wardlaw, A.J. (2005). Expression of CXCR6 and its ligand CXCL16 in the lung in health and disease. Clin. Exp. Allergy *35*, 1572–1580.

49. Gupta, A., Madhavan, M.V., Sehgal, K., Nair, N., Mahajan, S., Sehrawat, T.S., Bikdeli, B., Ahluwalia, N., Ausiello, J.C., Wan, E.Y., et al. (2020). Extrapulmonary manifestations of COVID-19. Nat. Med. *26*, 1017–1032.

50. Gu, J., Gong, E., Zhang, B., Zheng, J., Gao, Z., Zhong, Y., Zou, W., Zhan, J., Wang, S., Xie, Z., et al. (2005). Multiple organ infection and the pathogenesis of SARS. J. Exp. Med. *202*, 415–424.

51. Ding, Y., He, L., Zhang, Q., Huang, Z., Che, X., Hou, J., Wang, H., Shen, H., Qiu, L., Li, Z., et al. (2004). Organ distribution of severe acute respiratory syndrome (SARS) associated coronavirus (SARS-CoV) in SARS patients: implications for pathogenesis and virus transmission pathways. J. Pathol. *203*, 622–630.

52. Babel, N., Anft, M., Blazquez-Navarro, A., Doevelaar, A.A.N., Seibert, F.S., Bauer, F., Rohn, B.J., Hoelzer, B., Thieme, C.J., Roch, T., et al. (2020). Immune monitoring facilitates the clinical decision in multifocal COVID-19 of a pancreas-kidney transplant patient. Am. J. Transplant. Published online August 10, 2020. https://doi.org/10.1111/ajt.16252.

53. Westhoff, T.H., Seibert, F.S., Bauer, F., Stervbo, U., Anft, M., Doevelaar, A.A.N., Rohn, B.J., Winnekendonk, G., Dittmer, U., Schenker, P., et al. (2020). Allograft infiltration and meningoencephalitis by SARS-CoV-2 in a pancreas-kidney transplant recipient. Am. J. Transplant. Published online July 26, 2020. https://doi.org/10.1111/ajt.16223.

54. Matheson, N.J., and Lehner, P.J. (2020). How does SARS-CoV-2 cause COVID-19? Science *369*, 510–511.

55. Chen, Z., and John Wherry, E. (2020). T cell responses in patients with COVID-19. Nat. Rev. Immunol. *20*, 529–536.

56. Lucas, C., Wong, P., Klein, J., Castro, T.B.R., Silva, J., Sundaram, M., Ellingson, M.K., Mao, T., Oh, J.E., Israelow, B., et al.; Yale IMPACT Team (2020). Longitudinal analyses reveal immunological misfiring in severe COVID-19. Nature *584*, 463–469.

57. Cavalli, G., De Luca, G., Campochiaro, C., Della-Torre, E., Ripa, M., Canetti, D., Oltolini, C., Castiglioni, B., Din, C.T., Boffii, N., et al. (2020). Interleukin-1 blockade with high-dose anakinra in patients with COVID-19, acute respiratory distress syndrome, and hyperinflammation: a retrospective cohort study. Lancet Rheumatol *2*, E325–E331, https://doi.org/10.1016/S2665-9913(20)30127-2.

58. Mourad, J.-J., and Azria, P. (2020). Tocilizumab for severe COVID-19 pneumonia. Lancet Rheumatol. Published online August 17, 2020. https://doi.org/10.1016/S2665-9913(20)30282-4.

59. Nienen, M., Stervbo, U., Mölder, F., Kaliszczyk, S., Kuchenbecker, L., Gayova, L., Schweiger, B., Jürchott, K., Hecht, J., Neumann, A.U., et al. (2019). The role of pre-existing cross-reactive central memory CD4 T-cells in vaccination with previously unseen influenza strains. Front. Immunol. *10*, 593.

60. Ahmed, S.F., Quadeer, A.A., and McKay, M.R. (2020). preliminary identification of potential vaccine targets for the COVID-19 coronavirus (SARS-CoV-2) based on SARS-CoV immunological studies. Viruses *12*, 254.

61. Mueller, K., Schachtner, T., Sattler, A., Meier, S., Friedrich, P., Trydzenskaya, H., Hinrichs, C., Trappe, R., Thiel, A., Reinke, P., and Babel, N. (2011). BK-VP3 as a new target of cellular immunity in BK virus infection. Transplantation *91*, 100–107.

62. R Core Team (2020). R: A Language and Environment for Statistical Computing (R Foundation for Statistical Computing), http://www.R-project.org/.

63. Li, G., Taljaard, M., Van den Heuvel, E.R., Levine, M.A.H., Cook, D.J., Wells, G.A., Devereaux, P.J., and Thabane, L. (2017). An introduction to multiplicity issues in clinical trials: the what, why, when and how. Int. J. Epidemiol. *46*, 746–755.

YMTHE, Volume *28*

Supplemental Information

COVID-19-Induced ARDS Is Associated with Decreased Frequency of Activated Memory/Effector T Cells Expressing CD11a^{++}

Moritz Anft, Krystallenia Paniskaki, Arturo Blazquez-Navarro, Adrian Doevelaar, Felix S. Seibert, Bodo Hölzer, Sarah Skrzypczyk, Eva Kohut, Julia Kurek, Jan Zapka, Patrizia Wehler, Sviatlana Kaliszczyk, Sharon Bajda, Constantin J. Thieme, Toralf Roch, Margarethe Justine Konik, Marc Moritz Berger, Thorsten Brenner, Uwe Kölsch, Toni L. Meister, Stephanie Pfaender, Eike Steinmann, Clemens Tempfer, Carsten Watzl, Sebastian Dolff, Ulf Dittmer, Mohamed Abou-El-Enein, Timm H. Westhoff, Oliver Witzke, Ulrik Stervbo, and Nina Babel

Supplemental Appendix

Table of Contents

Supplement tables

Table S1. Clinical characteristics of the study patients according to disease severity

	Disease Severity		P value
	COVID-19 Control	ARDS	
Number of Patients	35 (77.8%)	10 (22.2%)	-
Chest CT abnormalities			
Bilateral ground-glass opacity	28 (80.0%)	10 (100.0%)	0.320
Pleural effusion	2 (5.7%)	1 (10.0%)	0.539
Median laboratory findings			
pO2/FiO2 mmHg	NA	129 [86-166.75]	-
Platelets (cells/nL)	179 [160.5-266.5]	189.5 [149.25-249.5]	0.827
Hemoglobin (g/dL)	12.7 [11.9-14.25]	8.85 [8.425-9.2]	<0.001
C-reactive protein (mg/dL)	8.9 [4.65-13.75]	15.4 [11-27]	0.015
Procalcitonin (ng/mL)	0.065 [0.02-0.265]	2.425 [1.405-3.37]	<0.001
Lactate dehydrogenase (U/L)	305 [272.5-396]	469.5 [357-584]	0.013
Total bilirubin (mg/dL)	0.6 [0.3-0.9]	1.5 [1.1-2.675]	<0.001
GFR (mL/min/1.73m^2)	46 [41.975-53.5]	45.9 [39-50]	0.935
Therapy			
Oxygen	19 (54.3%)	10 (100.0%)	0.008
Intravenous antibiotics	26 (74.3%)	10 (100.0%)	0.173
Admission to intensive care unit	0 (0.0%)	10 (100.0%)	<0.001
Mechanical Ventilation	0 (0.0%)	10 (100.0%)	<0.001
Hydrocortisone	1 (2.9%)	1 (10.0%)	0.399
Hydroxychloroquine	1 (2.9%)	6 (60.0%)	<0.001
Aciclovir	0 (0.0%)	1 (10.0%)	0.222
Outcome			
Length of hospitalization (days)	11 [7-26.5]	39 [34.75-43.5]	0.016
Currently hospitalized	4 (11.4.0%)	0 (0.0%)	1.000
Death	0 (0.0%)	6 (60.0%)	<0.001
Discharge	31 (88.6%)	4 (40.0%)	0.004

Quantitative variables are expressed as median [IQR] and compared by the Kruskal-Wallis test. Categorical variables are compared employing Fisher's exact test. GFR estimated by MDRD. NA: indicate not applicable

Table S2. Association of sex with the potential markers of COVID-19 severity

Cell population	P value sex	P value ARDS
Lymphocytes (cells/nL)	0.188	0.038
$CD3^+$ (cells/nL)	0.173	0.066
NK cells (cells/nL)	0.866	0.044
Eosinophil cells	0.230	0.017
% CM among $CD4^+$	0.072	0.004
% $CD4^+HLA\text{-}DR^+$ among $CD4^+$	0.724	0.036
% $CD8^+HLA\text{-}DR^+$ among $CD8^+$	0.582	0.010
% $CD4^+CD11a^{++}$ among $CD4^+$	0.010	0.074
% $CD8^+CD11a^{++}$ among $CD8^+$	0.094	<0.001
% $CD4^+CD28^+$ among $CD4^+$	0.167	<0.001
% Transitional among $CD19^+$	0.497	0.197
% Anti-S $CD4^+CD154^+$	0.691	0.040
% Anti-S $CD8^+CD137^+$	0.985	0.058
% Anti-S $CD8^+CD137^+IFN\gamma^+$	0.882	0.049
% Anti-S $CD4^+CD154^+IL\text{-}2^+$	0.601	0.066
% Anti-S $CD8^+CD137^+IL\text{-}2^+$	0.835	0.059
% Anti-S $CD8^+CD137^+TNF\alpha^+$	0.188	0.038

Association of sex with potential markers of COVID-19 severity at the initial visit was assessed by bivariate regression.

Table S3. Frequency of patients with detectable antigen specific T cell subpopulations

			Disease Severity		
T cell subpopulation	Visit	All patients	COVID-19 Control	ARDS	P value
$CD4^+CD154^+$	Initial	18 (66.7%)	10 (58.8%)	8 (80.0%)	0.406
	Follow-up	16 (100.0%)	12 (100.0%)	4 (100.0%)	-
$CD4^+CD154^+GrB^+$	Initial	11 (40.7%)	8 (47.1%)	3 (30.0%)	0.448
	Follow-up	5 (31.2%)	4 (33.3%)	1 (25.0%)	1.000
$CD4^+CD154^+IFN\gamma^+$	Initial	18 (66.7%)	11 (64.7%)	7 (70.0%)	1.000
	Follow-up	13 (81.2%)	9 (75.0%)	4 (100.0%)	0.529
$CD4^+CD154^+IL2^+$	Initial	19 (70.4%)	10 (58.8%)	9 (90.0%)	0.190
	Follow-up	14 (87.5%)	10 (83.3%)	4 (100.0%)	1.000
$CD4^+CD154^+TNF\alpha^+$	Initial	18 (66.7%)	10 (58.8%)	8 (80.0%)	0.406
	Follow-up	14 (87.5%)	10 (83.3%)	4 (100.0%)	1.000
$CD8^+CD137^+$	Initial	15 (55.6%)	7 (41.2%)	8 (80.0%)	0.107
	Follow-up	9 (56.2%)	5 (41.7%)	4 (100.0%)	0.088
$CD8^+CD137^+GrB^+$	Initial	15 (55.6%)	8 (47.1%)	7 (70.0%)	0.424
	Follow-up	8 (50.0%)	5 (41.7%)	3 (75.0%)	0.569
$CD8^+CD137^+IFN\gamma^+$	Initial	10 (37.0%)	4 (23.5%)	6 (60.0%)	0.101
	Follow-up	8 (50.0%)	4 (33.3%)	4 (100.0%)	0.077
$CD8^+CD137^+IL2^+$	Initial	8 (29.6%)	2 (11.8%)	6 (60.0%)	0.025
	Follow-up	5 (31.2%)	2 (16.7%)	3 (75.0%)	0.063
$CD8^+CD137^+TNF\alpha^+$	Initial	8 (29.6%)	3 (17.6%)	5 (50.0%)	0.102
	Follow-up	3 (18.8%)	2 (16.7%)	1 (25.0%)	1.000

The presence of SARS-CoV-2-reactive T cells was evaluated in 27 patients at the initial visit (17 COVID-19 Control and 10 ARDS) and 16 at follow-up (12 COVID-19 Control and 4 ARDS). Differences between patient groups for initial and follow-up for each T-cell subpopulation are calculated by Fisher's exact test.

Table S4. Frequency of patients with detectable polyfunctional SARS-CoV-2 reactive T cells

	Number of expressed cytokines	Initial		P value	Follow-Up		P value
		COVID-19 Control	ARDS		COVID-19 Control	ARDS	
$CD4^+$ T cells	1	94.1% (16/17)	100% (10/10)	1.000	100% (17/17)	100% (4/4)	1.000
	2	70.6% (12/17)	100% (10/10)	0.124	82.4% (14/17)	100% (4/4)	1.000
	3	52.9% (9/17)	50% (5/10)	1.000	52.9% (9/17)	100% (4/4)	0.131
	4	29.4% (5/17)	10% (1/10)	0.355	23.5% (4/17)	25% (1/4)	1.000
$CD8^+$ T cells	1	100% (17/17)	100% (10/10)	1.000	76.5% (13/17)	100% (4/4)	0.546
	2	70.6% (12/17)	90% (9/10)	0.363	70.6% (12/17)	100% (4/4)	0.532
	3	23.5% (4/17)	50% (5/10)	0.219	23.5% (4/17)	75% (3/4)	0.088
	4	0% (0/17)	10% (1/10)	0.393	17.6% (3/17)	25% (1/4)	1.000

Percentage (number) of patients with detectable polyfunctional SARS-CoV-2-reactive T cells. Differences between patient groups for initial and follow-up are calculated by Fisher's exact test.

Supplement figures

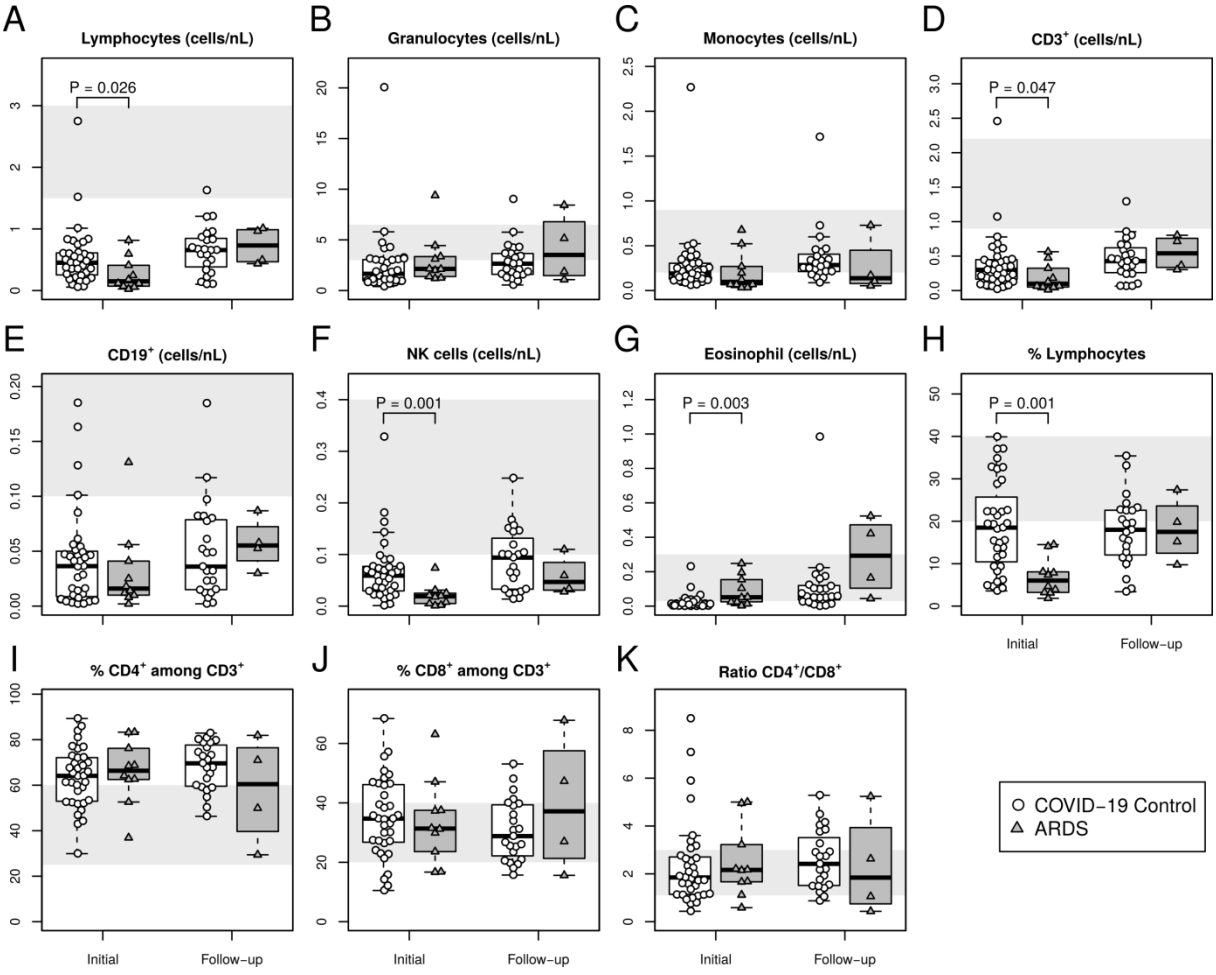

Figure S1. ARDS is associated with severe lymphopenia.

Circulating immune cell subsets were characterized in patients confirmed COVID-19 at the initial visit using multiparametric flow cytometry. In total, 45 patients from the COVID-19 Control (n=35, in white) or ARDS (n=10, in gray) sub-cohorts were analyzed at the initial visit and at follow-up. In all cases, the left boxplots show the data for the initial visit, while the right boxplots depict the data at follow-up. Immune cell subsets in peripheral blood were evaluated according to the gating strategy in Fig. S8. Cell counts were evaluated for (A) Lymphocytes, defined as $CD45^{+}SSC^{low}$, (B) Granulocytes, defined as $CD45^{+}SSC^{high}$, and (C) Monocytes, defined as $CD45^{+}SSC^{intermediate}$. Within the lymphocytes the cell counts were assessed for (D) T cells, defined as $CD3^{+}$ lymphocytes, (E) B cells, defined as $CD19^{+}CD3^{-}$, (F) natural killer cells (NK), defined as $CD56^{+}CD3^{-}$. (G) The cell counts of the Granulocyte subpopulation Eosinophils, defined as $CD45^{+}SSC^{high}CD16^{-}$. The frequency of (H) lymphocytes in whole blood, (I) T helper cells, defined as $CD3^{+}CD4^{+}CD8^{-}$ and (J) cytotoxic T cells identified as $CD3^{+}CD8^{+}CD4^{-}$ among $CD3^{+}$ T cells. (K) Ratio of $CD4^{+}$ and $CD8^{+}$ T cells in I and J. The shaded area indicates the reference range in healthy individuals.

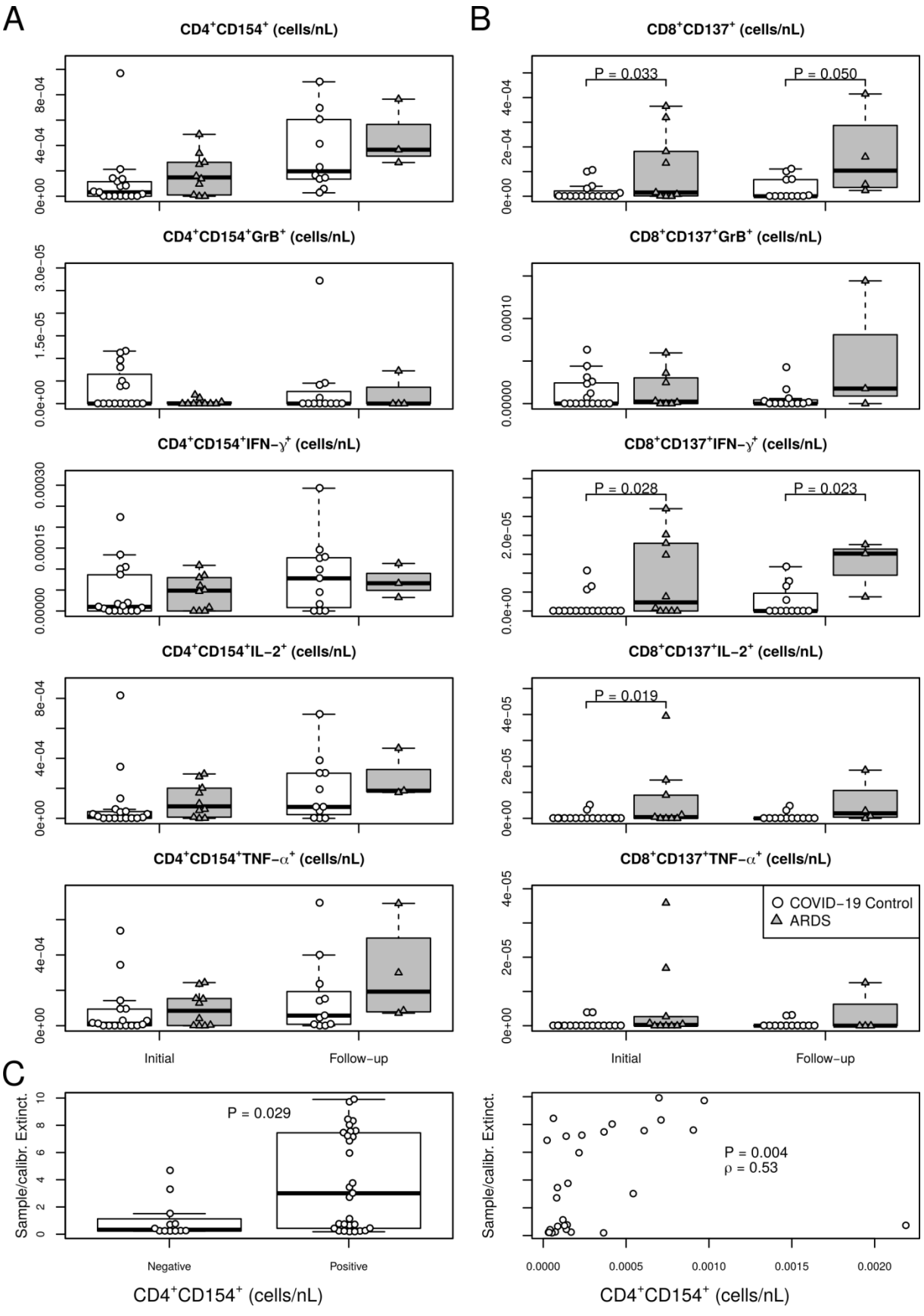

Figure S2 Increased number and functional activity of SARS-CoV-2-reactive T cells in ARDS patients.

The presence and functional status of SARS-CoV-2-reactive T cells was evaluated using PBMCs, isolated from the peripheral blood of 27 patients (17 COVID-19 Control, in white, and 10 ARDS, in gray). Defrosted PBMCs rested for 24 hours before treatment with overlapping peptide pools covering the SARS-CoV-2 S-protein. The cells were stimulated for a total of 16 hours and in the presence of Brefeldin A for the last 14 hours. The complete gating strategy is presented in Fig. S7. (A) $CD4^+CD154^+$ counts (first row) for ARDS and COVID-19 Control patients at the initial visit (left boxplots) and follow-up (right boxplots), and counts of $CD4^+CD154^+$ cells expressing granzyme B (GrB), INF-γ, IL-2, and TNF-α (row two to four). (B) $CD8^+CD137^+$ counts (first row) for ARDS and COVID-19 Control patients at the initial visit (left boxplots) and follow-up (right boxplots), and counts of $CD8^+CD137^+$ cells expressing granzyme B (GrB), INF-γ, IL-2, and TNF-α among (row two to four). (C) Comparison of the relative titers of SARS-CoV-2 S-protein specific IgG antibodies, measured by ELISA and evaluated as ratio to an internal control for samples with detectable SARS-CoV-2 specific $CD4^+$ T cells (left) and cellcorrelation of the relative titers of SARS-CoV-2 with the counts of SARS-CoV-2 specific $CD4^+$ T cells (right) cell. Note that no measurements of IgG antibodies were available for ARDS patients.

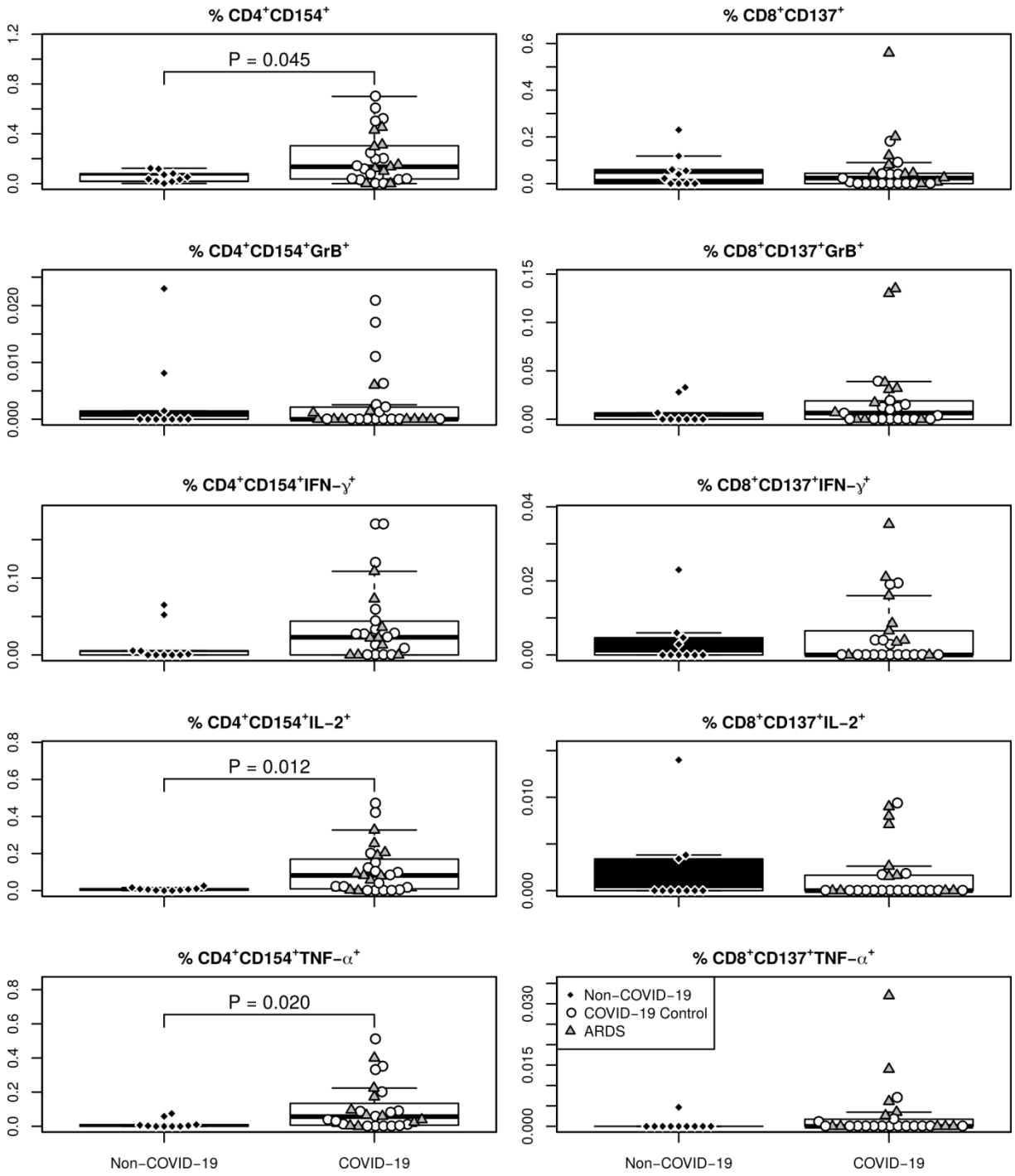

Figure S3. Increased frequency and functional activity of SARS-CoV-2-reactive T cells in COVID-19 patients compared to COVID-19 unexposed healthy blood donors.

The presence and functional status of SARS-CoV-2-reactive T cells was evaluated in COVID-19 unexposed healthy donors in comparison to the cohort of COVID-19 patients. For the unexposed patients, blood samples were collected before pandemics onset and stored at -80°C. For COVID-19 cohort, the last available sample per patient was included in the analysis. The complete gating strategy is presented in Fig. S6.

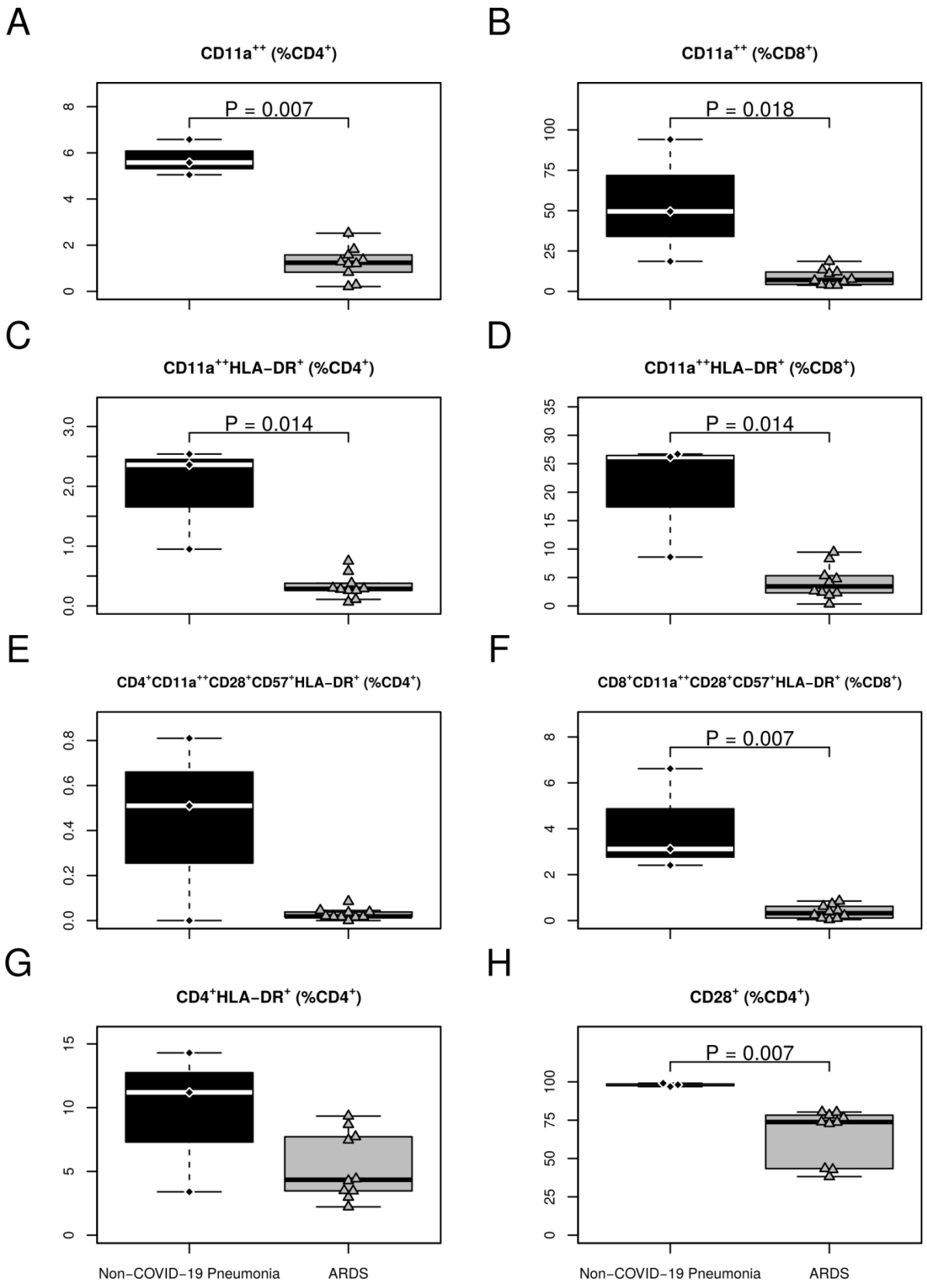

Figure S4. The observed alterations of T cell subsets for ARDS patients were COVID-specific

Potential markers of COVID-19 severity were analyzed for their specificity. Peripheral blood from patients with COVID-19-associated ARDS (ARDS, n=10, in gray) and patients with non-COVID-19 pneumonia and sepsis on mechanical ventilation (Non-COVID-19 Pneumonia, n=3, in gray) at the initial visit was subjected to evaluation for differentiation and activation state of T- cell using multiparametric flow cytometry. The subsets of the $CD3^+$ T cells were identified according to the gating strategy in Fig. S9 and S10. (A-B) The frequency of $CD11a^{++}$ cells among $CD4^+$ (A) and $CD8^+$ (B) $CD3^+$ T cells. (C-D) The frequency of $CD11a^{++}HLA\text{-}DR^+$ expressing cells among $CD4^+$ (C) and $CD8^+$ (D) $CD3^+$ T cells. (E-F) The frequency of $CD11a^{++}HLA\text{-}DR^+CD28^+CD57^+$ expressing cells among $CD4^+$ (E) and $CD8^+$ (F) $CD3^+$ T cells. (G) Expression of HLA-DR among and $CD4^+$ T cells. (H) Expression of CD28 among $CD4^+$ T cells.

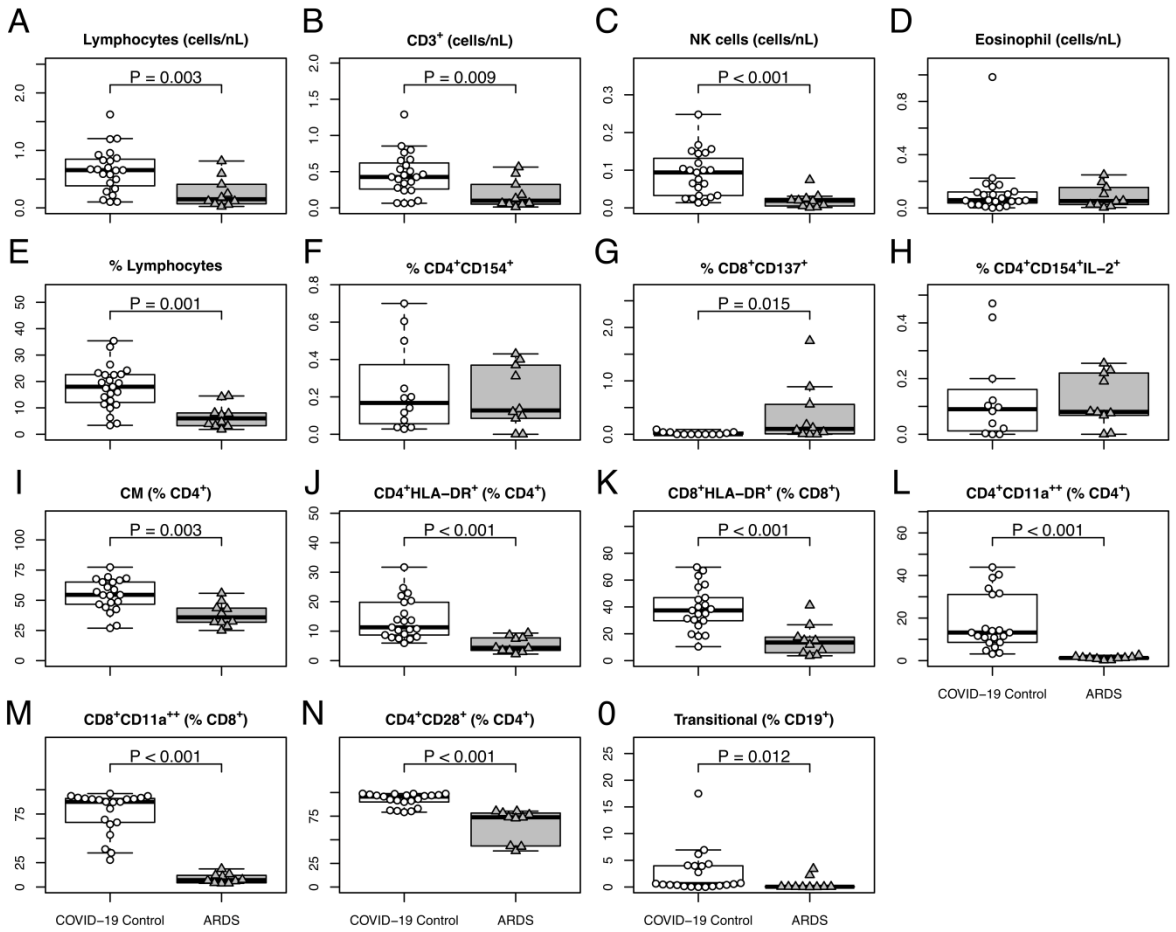

Figure S5. The observed immunological alterations for ARDS patients were not due to the differences in sampling time

To demonstrate that the observed results are not due to the differences in sampling time, we additionally performed analyses using samples of both groups obtained at similar time points in days after initial diagnosis (7 [3-10] for COVID-19 control vs. 8 [6-15] days in ARDS cohort; P=0.766). The comparison was performed for all markers that showed a significant effect of ARDS at the initial visit (Figures S1, 2 and 3). ARDS patients (n=10, in gray) were compared with the COVID-19 Control patients (n=23, in white). The subsets were identified according to the gating strategies in Fig. S6-10. (A-D) The counts of lymphocytes, $CD3^+$ cells, NK cells and eosinophils and (E) the frequency of lymphocytes. (F-H) Frequency of SARS-CoV-2-reactive $CD4^+CD154^+$, $CD8^+CD137^+$ cells and IL-2-secreting $CD4^+CD154^+$ cells. (I-O) Frequency of CM $CD4^+$, $CD4^+$HLA-DR^+, $CD8^+$HLA-DR^+, $CD4^+CD11a^{++}$, $CD8^+CD11a^{++}$, $CD4^+CD28^+$ and transitional B cells.

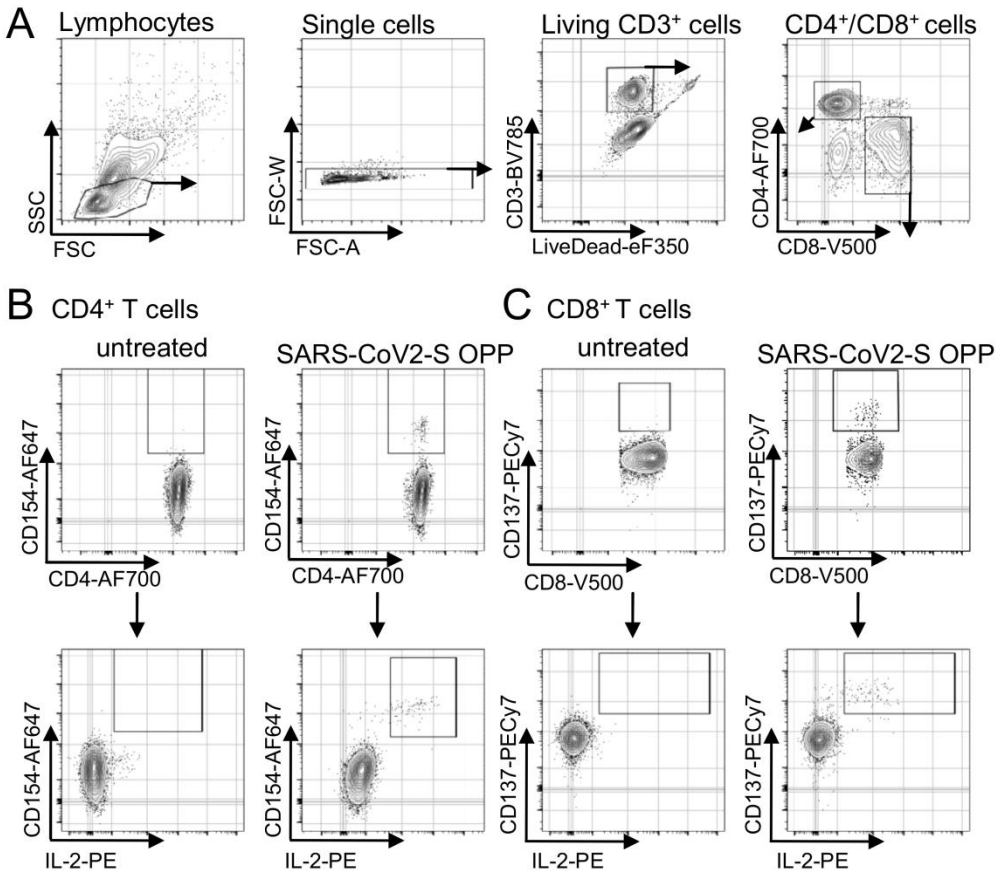

Figure S6. Gating strategy for detection of cytokine producing $CD4^+$ and $CD8^+$ antigen specific T cells.

Isolated PBMCs were stimulated with SARS-CoV-2 spike protein OPPs or left untreated for 16h. (A) Lymphocytes were gated based on side and forward scatter profile, doublets were excluded and living T cells were identified as $CD3^+$ and Live/Dead-Marker negative cells, expressing either CD4 or CD8. Antigen specific T cells were identified as $CD4^+CD154^+CD137^+$ T-helper cells (B) or $CD8^+CD137^+$ cytotoxic T cells (C). Within the antigen specific T cells, intracellular staining of cytokines and granzyme B was used to identify effector cells.

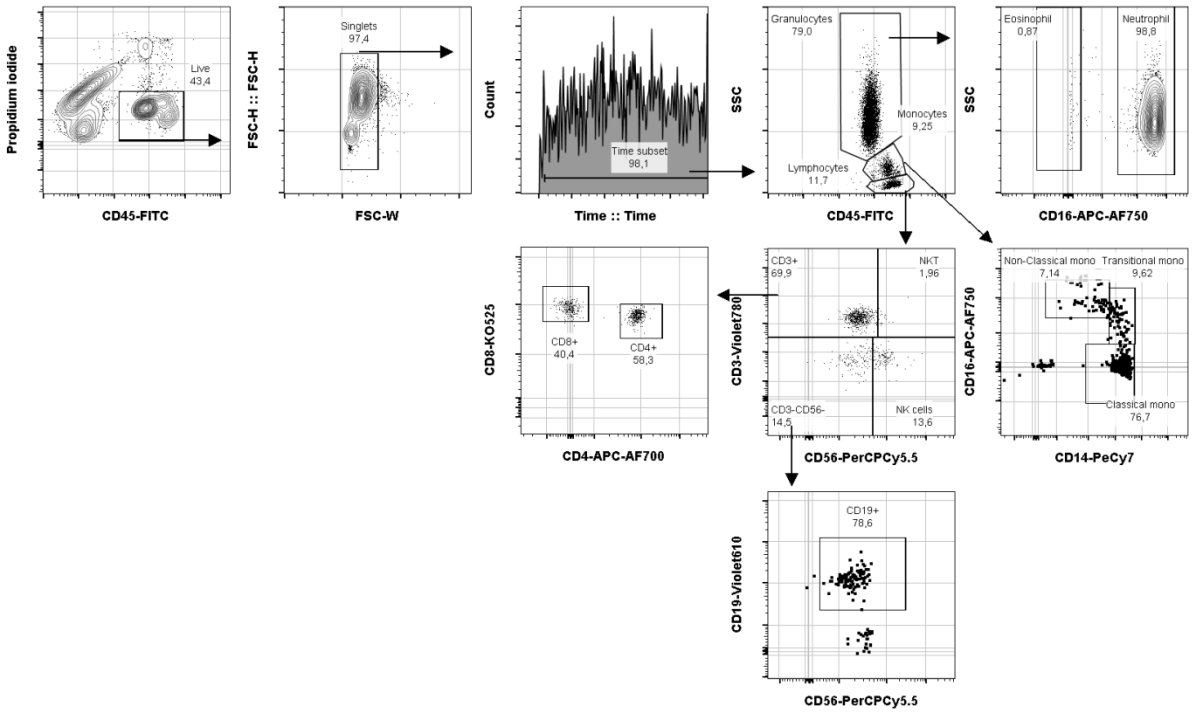

Figure S7. Gating strategy for identification of main immune cell populations.

Whole blood was diluted 1:1 in staining solution prior to erythrocytes lysis. Live cells were identified as negative for propidium iodide and doublets were excluded. Granulocytes, monocytes and lymphocytes were distinguished by CD45 and side scatter profile. Granulocytes were separated by CD16 in Eosinophiles ($CD16^{-}$) and Neutrophiles ($CD16^{+}$). Monocytes were divided by the expression of CD14 and CD16 into classical- ($CD14^{++}CD16^{-}$), intermediate- ($CD14^{++}CD16^{+}$) and non-classical Monocytes ($CD14^{+}CD16^{+}$). Lymphocytes were separated by CD3 and CD56 in NK ($CD3^{-}CD56^{+}$), NKT ($CD3^{+}CD56^{+}$) and T cells ($CD3^{+}CD56^{-}$) and T cells were further distinguished into $CD4^{+}$ helper T cells and $CD8^{+}$ cytotoxic T cells. B cells were identified as CD3/CD56 double negative and CD19 positive cells.

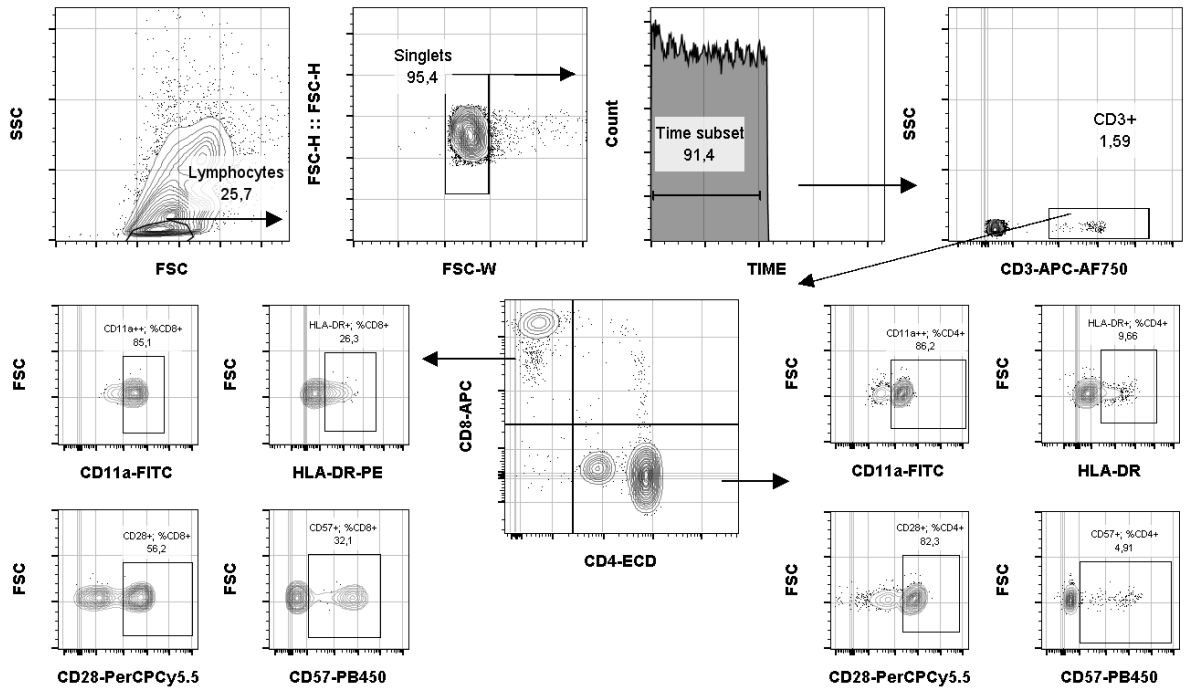

Figure S8. Gating strategy for identification of activated T cells.

Whole blood was diluted 1:1 in staining solution prior to erythrocytes lysis. Living lymphocytes were identified by their forward and sideward scatter profile and doublets were excluded. T cells were identified as $CD3^+$ and separated by expression of CD4 and/or CD8 into double negative ($CD4^-CD8^-$), double positive ($CD4^+CD8^+$), T-helper cells ($CD4^+CD8^-$) and cytotoxic T cells ($CD4^-CD8^+$). The expression of activation marker CD11a, HLA-DR, CD28 and CD57 was assessed on $CD4^+$ and $CD8^+$ single positive T cells.

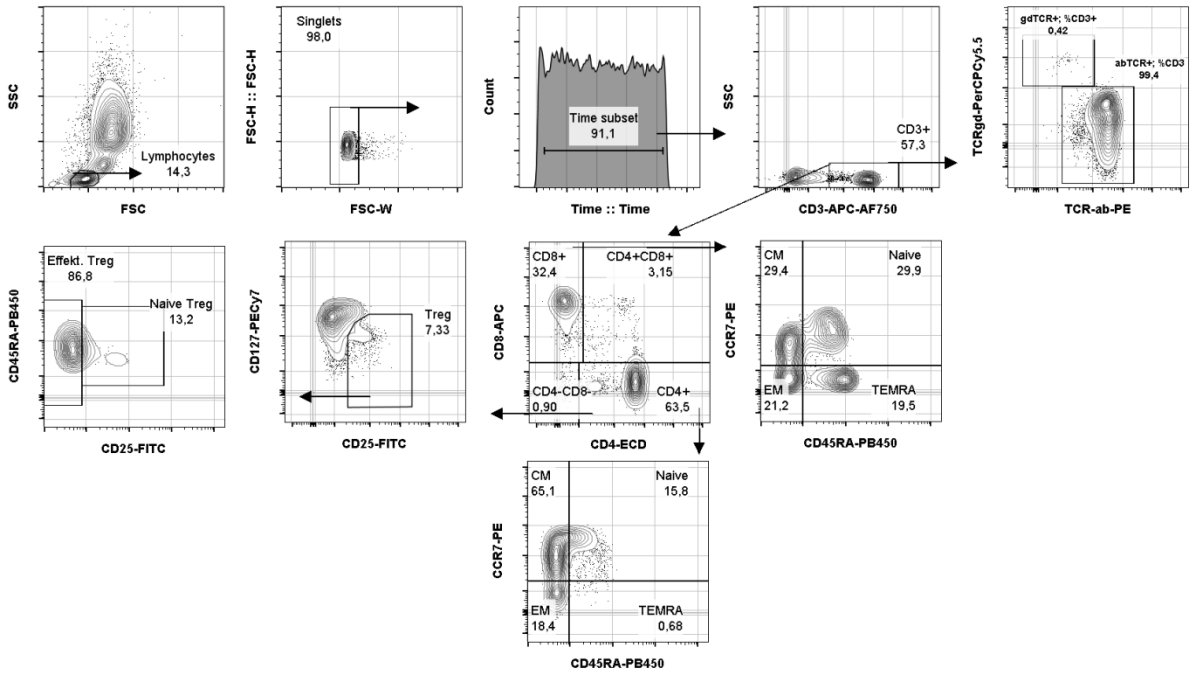

Figure S9. Gating strategy for identification of memory and regulatory T cells.

Whole blood was diluted 1:1 in staining solution prior to erythrocytes lysis. Living lymphocytes were identified by their forward and sideward scatter profile and doublets were excluded. T cells were identified by the expression of CD3 and separated into αβ-T cells and γδ-T cells by staining with TCR antibodies against TCRαβ and TCRγδ antibodies. Additionally, $CD3^+$ T cells were divided into T-helper cells ($CD4^+CD8^-$) and cytotoxic T cells ($CD4^-CD8^+$). Both T cell subsets were further divided by the expression of CD45RA and CCR7 into naïve ($CD45RA^+CCR7^+$), central memory (CM, $CD45RA^-CCR7^+$), effector memory (EM, $CD45RA^-CCR7^-$) and T effector RA (TEMRA, $CD45RA^+CCR7^-$) T cells. Additionally, regulatory T cells (Tregs) were identified as $CD4^+CD25^+CD127^+$ and further separated by their expression of CD45RA into Naïve ($CD45RA^+$) and effector Tregs ($CD45RA^-$).

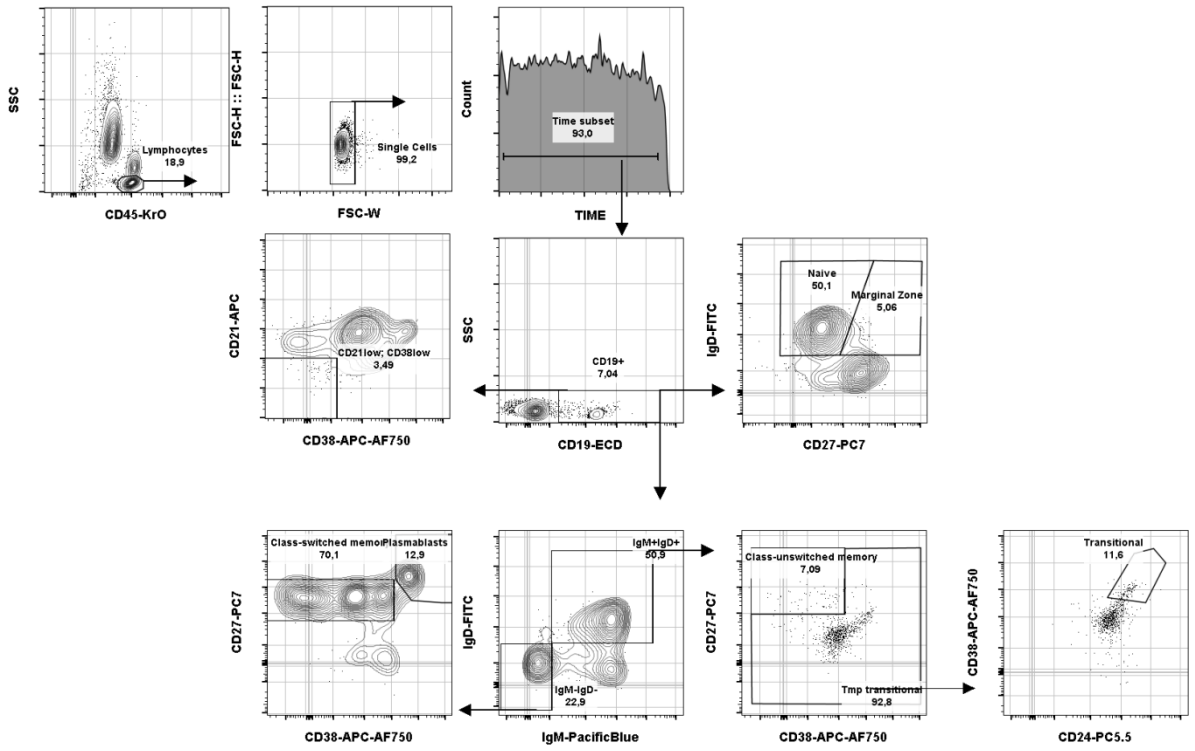

Figure S10. Gating strategy for identification of B cell subpopulations.

Whole blood was diluted 1:1 in staining solution and afterwards erythrocytes were lysed. Living lymphocytes were identified by their forward and sideward scatter profile and doublets were excluded. B cells were identified by the expression of CD19 and separated into naïve ($IgD^{+}CD27^{-}$), marginal zone B cells ($IgD^{+}CD27^{+}$) and $CD21^{low}CD38^{low}$ B cells. Additionally, B cells were separated by expression of IgM and IgD into double negative ($IgM^{-}IgD^{-}$) and double positive ($IgM^{+}IgD^{+}$) cells. Double negative cells could be separated by CD38 and CD27 into class-switch memory B cells and Plasmablasts ($CD27^{high}CD38^{high}$). IgM/IgD double positive B cells were further divided into class-unswitched memory B cells ($CD27^{+}CD38^{-}$) and $CD38^{high}CD24^{high}$ transitional B cells.